Bureau of Safety and Environmental Enforcement
Oil Spill Preparedness Division

Efficient Remediation of Oil Spills Using Fire Whirls

Final Report

January 2024

(Photo: Wuquan Cui, 2023)

Michael Gollner, Elaine Oran, Qingsheng Wang, Mohammadhadi Hajilou, Joseph Dowling, Wuquan Cui

US Department of the Interior
Bureau of Safety and Environmental Enforcement
Oil Spill Preparedness Division

Efficient Remediation of Oil Spills Using Fire Whirls

Final Report

OSRR # 1124

January 2024

Authors:
Michael Gollner
University of California, Berkeley

Elaine Oran
Texas A&M University

Qingsheng Wang
Texas A&M University

Mohammadhadi Hajilou
University of California, Berkeley

Joseph Dowling
University of California, Berkeley

Wuquan Cui
University of California, Berkeley

Prepared under Contract Number
140E0121C0004
By
University of California, Berkeley
University Avenue, Berkeley, CA 94720

US Department of the Interior
Bureau of Safety and Environmental Enforcement
Oil Spill Preparedness Division

DISCLAIMER

Contracts:

Study concept, oversight, and funding were provided by the US Department of the Interior (DOI), Bureau of Safety and Environmental Enforcement (BSEE), Oil Spill Preparedness Division (OSPD), Sterling, VA, under Contract Number 140E0121C0004. This report has been technically reviewed by BSEE, and it has been approved for publication. The views and conclusions contained in this document are those of the authors and should not be interpreted as representing the opinions or policies of the US Government, nor does mention of trade names or commercial products constitute endorsement or recommendation for use.

REPORT AVAILABILITY

The PDF file for this report is available through the following sources. Click on the URL and enter the appropriate search term to locate the PDF:

Document Source	Search Term	URL
Bureau of Safety and Environmental Enforcement (BSEE)	Project Number – 1124	https://www.bsee.gov/what-we-do/research/oil-spill-preparedness/oil-spill-response-research
U.S. Department of the Interior Library	Efficient Remediation of Oil Spills Using Fire Whirls	https://library.doi.gov/uhtbin/cgisirsi/?ps=8L0mpW5uPV/SIRSI/X/60/495/X
National Technical Reports Library	Efficient Remediation of Oil Spills Using Fire Whirls	https://ntrl.ntis.gov/NTRL/

Sources: a) BSEE (2019), b) DOI [2021], c) National Technical Information Service (2021)

CITATION

Gollner M, Oran E, Wang Q, Hajilou M, Dowling J, Cui W (University of California, Berkeley, Berkeley CA). 2024. Efficient Remediation of Oil Spills Using Fire Whirls. Berkeley (CA). U.S. Department of the Interior, Bureau of Safety and Environmental Enforcement. Report No.: 1124. Contract No. 140E0121C0004.

ABOUT THE COVER

Cover image by Wuquan Cui / University of California, Berkeley. The photo was taken in the large-scale outdoor experiment conducted in this contract demonstrating the successful formation of large-scale fire whirl in an outdoor environment in cleaning spilled crude oil.

ACKNOWLEDGEMENTS

This study is funded by the Bureau of Safety and Environmental Enforcement (BSEE), U.S. Department of Interior, Washington, D.C., under contract number 140E0121C0004.

GRAPHICAL ABSTRACT

Efficient Remediation of Oil Spills Using Fire Whirls

Phase I

Fire whirl design

- A three-wall prototype developed
  - ✓ Three wall vs four wall
- Sizing effect investigated
  - ✓ Wall height
  - ✓ Air gap size
  - ✓ Center-to-wall distance

Diagnostics:
- Mass
- Temperature
- Heat flux
- Flow
- Gas
- PM

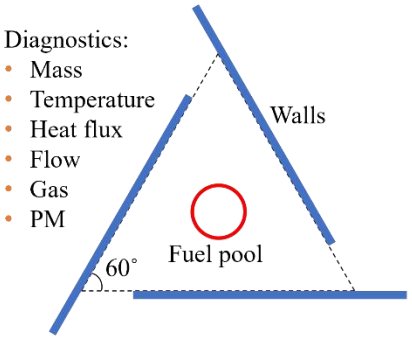

Phase II

Laboratory-scale experiments

- Fire whirl vs pool fire
- Slick thickness: 3.8 vs 7.6 vs 11.5 mm

Phase III

Large-scale outdoor experiments

- Fire whirl vs pool fire
- Slick thickness: 15 vs 40 mm

laboratory-scale vs large-scale

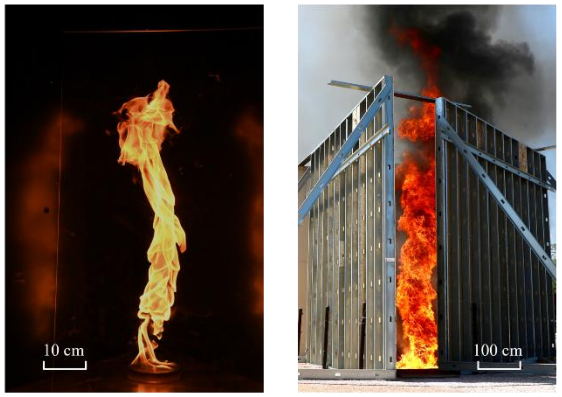

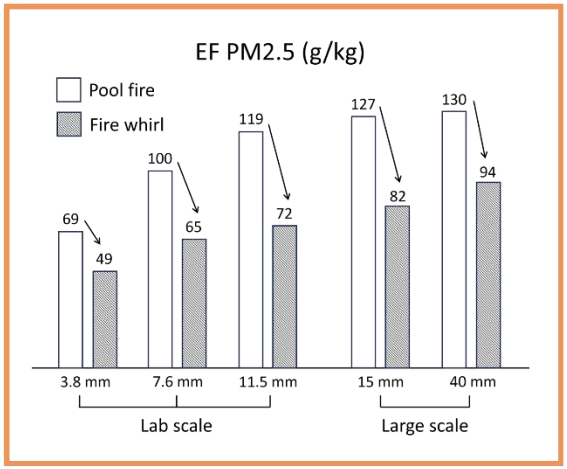

Berkeley Fire Research Lab
Dr. Michael J Gollner - mgollner@berkeley.edu

Berkeley UNIVERSITY OF CALIFORNIA | TEXAS A&M UNIVERSITY | BSEE Bureau of Safety and Environmental Enforcement

EXECUTIVE SUMMARY

In-situ burning (ISB) has been shown to be a reliable and effective response method to mitigate damage from oil spills on open water. Still, there are opportunities to improve burning efficiencies and further reduce adverse environmental impacts. Compared to traditional ISB using a pool fire configuration, fire whirls have been shown in laboratory studies to intensify the combustion process of oil spills and, under the right conditions, increase the burning efficiency and decrease atmospheric emissions. In this project, laboratory small-scale and outdoor large-scale experiments were performed to characterize the effects of fire whirls vs. pool fires and slick thickness on burning efficiencies and emissions. To generate fire whirls, a new three-wall geometry was developed where gaps between the walls were oriented to induce swirling at the center of the test section. Investigations were performed to assess the configuration and dimensions that can most effectively form fire whirls over liquid fuels at the laboratory scale, where systems with three or four walls were arranged to restrict airflow to the azimuthal direction around a central pool of n-heptane as a surrogate fuel. It was observed that the height and side length of the enclosure had an impact on the dynamics and formation of fire whirls, thus these parameters were varied compared to a fixed fuel pool diameter to assess any change in the flame length and burning rate. The optimal combinations of parameters from these experiments were then assessed in terms of their effects on particulate emissions and modified combustion efficiency. The obtained results in this study confirm the feasibility of using fire whirls with a three-wall setup for more efficient in-situ burning of crude oil spills and provide valuable information on the properties of fire whirls for deployment in the field. Furthermore, laboratory experiments were conducted to study the effect of slick thickness on the burning efficiency and emissions of crude oil. Experiments were done on three oil slick thicknesses, 3.8 mm (30 ml), 7.6 mm (60 ml) and 11.5 mm (90 ml), in a 10 cm diameter container with a water sublayer using HOOPS and ANS crude oil. The mass loss rate, gas and particle emissions, temperature of the oil and water sublayer, and flow rate and temperature of the effluence were measured for both pool fires and fire whirls. In addition, a large-scale experimental campaign was carried out at the TEEX Brayton Fire Training Field in Texas where we successfully conducted the largest to-date fire whirl experiments in an outdoor environment. Two oil slick thicknesses, 15 mm and 40 mm, were studied by using HOOPS crude oil, set inside a 1.5 m diameter metal ring suspended at the surface of a large water pool. Measurements included temperature measurements of the flame, oil layer and water layer, heat flux measurements near the pool center and on the side, air entrainment velocity, and particle and gas emissions. Videos were taken from four different angles and drone footage was taken from overhead during the experiments. At all scales we found that compared to pool fires, fire whirls significantly increased the burning rate, while also reducing PM2.5 emissions. By increasing the slick thickness from 3.8 mm to 11.5 mm in the laboratory, the burning rate increased more than 50% in fire whirls, with only a small change in pool fire conditions. Increasing the slick thickness in the laboratory also results in an increase in fuel consumption efficiency; nonetheless, it also increased emissions of PM2.5. In the field, fuel consumption efficiencies of over 90% could be reached, however, for many fire whirl tests premature extinguishment of the ISB was observed lowering ultimate fuel consumption efficiencies. These experiments have helped to provide experimental evidence assessing the scalability, robustness, and efficiency of fire whirls in cleaning spilled oil, and help to highlight issues on stability and premature extinguishment needing further study.

Contents

List of Figures

List of Tables

1 Introduction

1.1 Background

Marine activities such as oil exploration and extraction can cause accidental oil spills into inshore or offshore waters. Oil spills can pose a serious threat to surrounding populations (Gelderen and Jomaas 2017; van Gelderen et al. 2015), response workers (Law and Hellou 1999; Zock et al. 2007), and ecosystems (Law and Hellou 1999; Peterson et al. 2003; Teal and Howarth 1984). Additional effects include substantial disruption to local oil exploration infrastructure, marine transportation, and potentially widespread economic impacts (Fingas 2019). Rapidly advancing oil recovery technology as well as increased interests in local production continues to increase the probability of oil spills' occurrence (Peters 2017). In the case of such a spill, an efficient, effective, and robust treatment technique is crucial to mitigate their impact. In this regard, in-situ burning (ISB) is one of the most reliable and effective oil spill treatment techniques (Buist 2003; Fingas et al. 1995; Hobbs and Peter 1996), particularly in conditions where remoteness, harshness of the climate, and scale of the incident make it impossible for mechanical recovery or dispersant techniques to be deployed and utilized immediately after the spill. Fig. 1 below shows an example of ISB to clean oil spilled on the sea.

Fig. 1 ISB oil spill treatment
Image of a controlled in-situ burning (ISB) of an oil spill after the 2010 Deepwater Horizon/BP spill in the Gulf of Mexico. The dark plume of smoke indicates inefficient combustion and high levels of soot. (Photo: USCG, 2010)

Decades of laboratory and mesoscale testing of in-situ combustion of oil have shown that the composition and concentration of emitted emissions from in-situ burning (ISB) is an acceptable tradeoff in relation to inshore and offshore contamination and its environmental consequences and cleanup costs (Allen and Ferek 1993; Fingas et al. 1995). In fact, an efficient ISB has been shown to effectively eliminate at least 90% of the released liquid oil in some cases (Buist et al. 2011; Buist et al. 1997; Lin et al. 2005). ISB remains a fast and portable method of treating oil

spills, which is especially important as 70% of the untreated oil spills may emulsify during the first 24 hours (Bech et al. 1992; Buist 2003).

Despite their importance and effective use, ISB techniques are still challenged by the airborne emissions they release (especially near shore), oil slick thickness, the degree of weathering and emulsification, and the intensity of ambient wind and waves. In general, burns over water are oxygen-starved (Fingas 2019; IPIECA 2016); hence, ample black soot can be seen in almost any ISB. In fact, one of the major operational limits of current ISB practices is the after-burn emission concentrations, particularly at downwind distances close to populated areas. For instance, the maximum 1-hour averaged concentration of particulate matter of ten micrometers (PM_{10}) must not exceed 150 $\mu g/m^3$, according to ISB guidance from the National Response Team, Science and Technology Committee (National-Response-Team 1995). Reduction of PM requires high efficiency at the time of burning, including reaching ample oxygen concentrations, high temperatures over the fuel surface, and completeness of combustion (Fingas et al. 1995).

Our initial work has shown the reduction of PM and improvement of burning efficiency can be achieved using a phenomenon called the Fire Whirl (Hariharan et al. 2021). The fire whirl is one of the most dramatic structures which arises at the intersection of combustion and fluid dynamics, forming when the right conditions of wind and fire interact (Xiao et al. 2016). The resulting intensification of combustion imposes significantly higher heat feedback to the fuel surface, increasing the rate of burning, and has been shown in the earlier study to decrease the post-combustion residue, increase the amount of oxygen available to the fire causing higher temperatures within the fire, effectively reducing the emission of PM in the plume.

1.2 Motivation

There have been a number of prior studies of oil spreading on the sea (Fay 1969; Hoult 1972), and several of these have addressed the problems of burning spilled fuel (Cooperman 2004). During recovery efforts for accidental spills, the dispersed fuel is gathered using booms and ignited once the fuel layer is thick enough. This layer must be thick enough because it serves to insulate the top layer of fuel from the water. This entire approach is fundamentally different from traditional studies of pool fires burning lighter fuels over water (Ross 1994). Wu et al. (Wu et al. 1996) performed experiments to determine the ignition, flame spread, and mass burning characteristics of oil spilled on a water bed. Later, they expanded to more detailed ignition experiments determining the effects of weathering on crude oil (Wu et al. 1998), which is important because as oil becomes more weathered, it becomes more difficult to ignite, and finally it emulsifies to the point where ignition is no longer possible (Buist 2003). Based on these results, phenomenological descriptions have been developed for standard combustion of oil on water layer (Torero et al. 2003; Walavalkar and Kulkarni 2001). More recent experiments have measured the properties of crude oil layers and their effects, particularly applied to arctic regions (Brogaard et al. 2014). The initial concept for the first phase of the current line of investigation arose from observations of fire whirls that occurred naturally and accidentally in previous ISBs.

Previous experiments have shown that fire whirls result in cleaner, more efficient burning than pool fires (Gollner et al. 2019). Additionally, fuels were shown to burn at a higher rate than pool fires across scales, and at smaller scales where boil-over did not occur, the post-combustion

residue from fire whirls was lower than that from pool fires. Thus, if the formation and emissions from fire whirls in naturally entrained configurations can be optimized, there is the potential to improve existing ISB techniques by reducing burn times while also reducing the total amount of airborne particulate matter from ISBs.

1.3 Project Overview

The purpose of this study was to build on previous work and investigate fundamental and applied questions regarding fire whirl ISB. These will help in quantifying the potential reduction in particulate emissions by using fire whirl ISBs, and assist in the design of a reliable, controllable fire whirl ISB apparatus for cleaning up spilled oil. The specific objectives of this project were to:

- Characterize the ideal configurations and parameters for fire whirl formation
- Characterize the effects and burning/combustion efficiencies on emissions from different fire whirl configurations, fuels (such as ANS and HOOPS), and slick thicknesses
- Further understand the fundamental physics contributing to enhancements in the combustion efficiency of fire whirls vs. pool fires
- Develop a small or medium-scale prototype fire whirl generator for later use in a large-scale outdoor test facility
- Test the prototype developed in Phase 1 at an outdoor test facility at relevant scales (> 1 m diameter)
- Widely disseminate these results in publications, presentations, and media

The project was divided into three phases. *Phase I* dealt with understanding the fluid dynamics causing formation of fire whirls, focused on quantifying the influential scaling parameters that lead to reliable fire whirl formation under natural entrainment. This included Task 1: studying the sensitivity of fire whirl formation to enclosure dimensions and Task 2: developing a prototype and taking preliminary emissions measurements. *Phase II* sought to understand the effects of slick thickness on burning behavior and the steady-state burning effects on emissions from fire whirls and pool fires. Task 1 was to study the effect of crude oil slick thickness, in terms of burning behavior, efficiency and emissions for both ANS and HOOPS crude oil. Task 2 involved analyzing the data and disseminating information. Finally, based on results from the first two phases, a set of large-scale proof-of-concept experiments were conducted in *Phase III* using both ANS and HOOPS crude oil.

2 Laboratory Scale Experimental Setup

This chapter reviews the apparatus used to generate fire whirls, measurements in laboratory experiments, and related calibrations. A schematic of the experimental setup is shown in Fig. 2. A 10 cm diameter metal pan was used to contain water and fuel. Heptane and two different types of crude oils, ANS and HOOPS, were used in this project. The fire whirl apparatus was constructed using a three-wall structure developed in this project and placed over the pan. The results were compared to pool fire experiments with the same fuel pool. The fire whirl enclosure formed an equilateral triangle with a single gap on each side wall to allow for the tangential entrainment of air. This provided the air circulation needed to form the fire whirl over the fuel pool. The height of the walls was varied to find the best condition for fire whirls to form (results shown in Chapter 3). Each experiment used different volumes of fuel to study the effect of slick thickness on burning dynamics and emissions (results shown in Chapter 4).

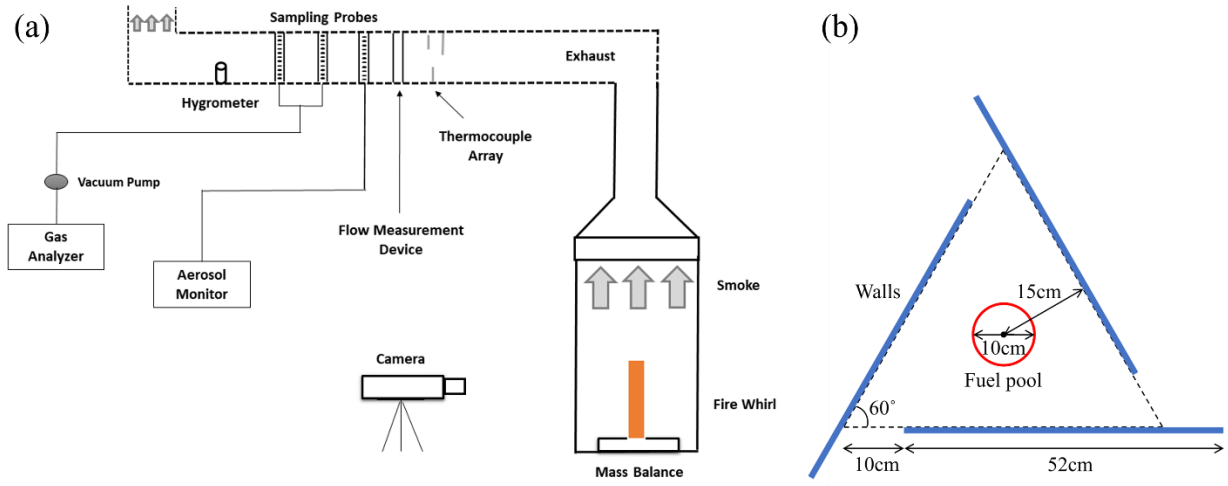

Fig. 2 Schematics of the experimental setup
Schematics showing the laboratory experimental setup: (a) side view with setups of instrumentations and (b) top view with dimensions of fire whirl structure.

A mass balance (Mettler Toledo) was used to track the instantaneous mass of the remaining fuel at a frequency of 1 Hz. The instantaneous mass of the remaining fuel was used to determine the average mass loss rate by fitting a linear function to the mass as a function of time, with the instantaneous mass loss rate calculated as the difference in mass over each second.

The experiments were conducted under an exhaust hood connected to an exhaust duct with a diameter of 23 cm (shown in Fig. 3(a)). A variable speed fan at the end of the duct could be adjusted to provide different flow velocities in the duct, where a flow measurement sensor (Veris Verabar V110) was used to account for the volumetric flow rate inside the duct. An array of three K-type thermocouples 305 cm downstream from the location of the exhaust duct were used to measure the average temperature of effluents in the duct. A photo of the completed exhaust measurement system is shown in Fig. 3(b). The gas velocity in the duct was verified using an anemometer 300 cm downstream of the exhaust hood to ensure a uniform velocity profile. The measured gas velocities at different radial distances from the bottom edge of the duct is shown in

Table 1. Based on these velocity measurements, it was observed that with the exhaust fan working at 50% of its capacity, the average velocity in the duct was 6.11 m/s, which translates into an average volumetric flow rate of 0.251 m^3/s.

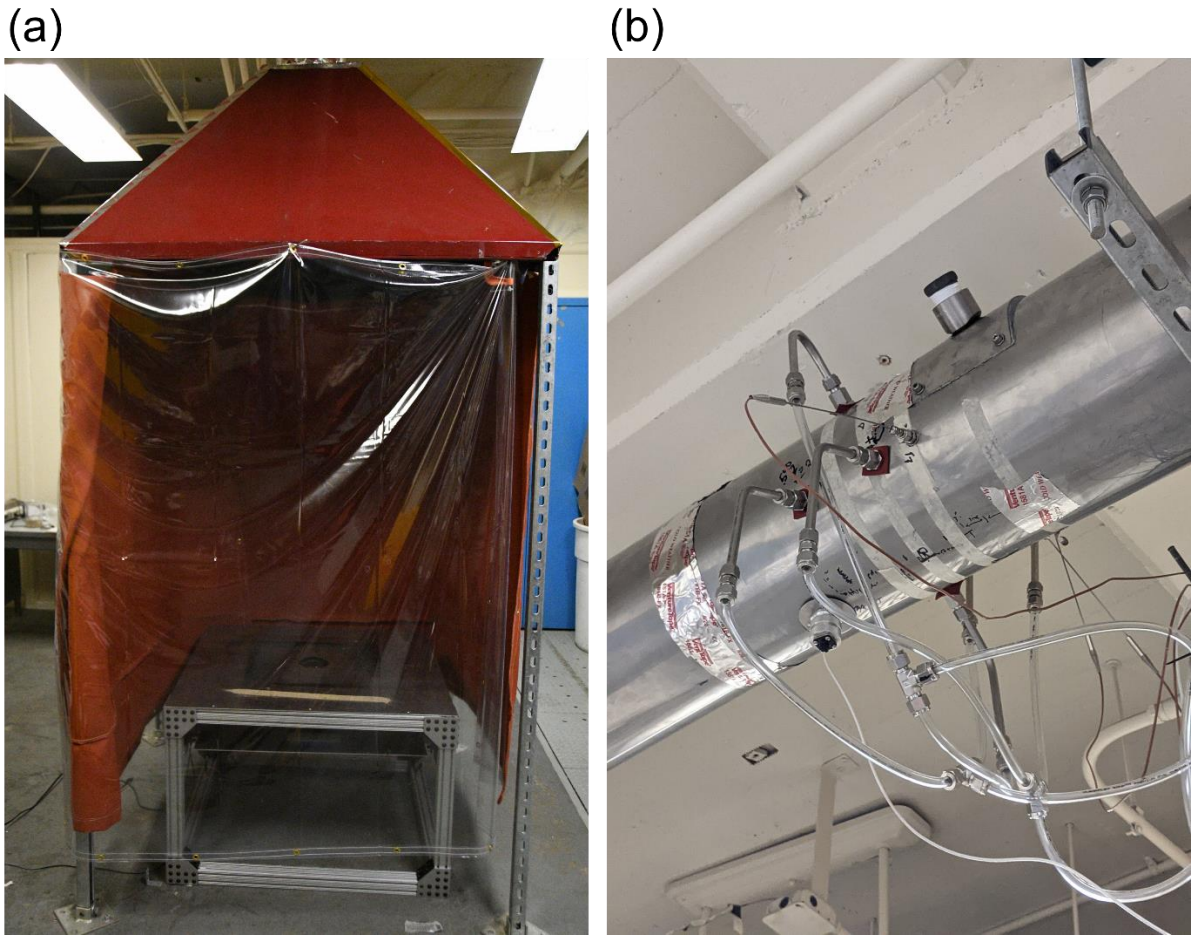

Fig. 3 Photos of the experimental setup
Photos showing the laboratory experimental setup: (a) setups of the exhaust hood and experimental bench; (b) setups of the exhaust duct along with instrumentations.

Table 1 Velocity measurements across the radial distance inside the exhaust duct

Radial distance (cm)	Velocity (m/s)
11.4	6.5
8.9	6.5
7.62	6.3
6.35	6
5.1	6
3.8	5.8
2.5	5.7

Additionally, the generated combustion effluents were sampled downstream of the thermocouple array using an optical aerosol monitor (TSI DustTrak DRX 8534) and a gas analyzer (CAI Instruments ZPA Model). The optical aerosol monitor was used to provide estimates of the concentrations of particles less than 2.5 micrometers in diameter ($PM_{2.5}$), while the gas analyzer was used to capture the concentrations of carbon monoxide (CO) and carbon dioxide (CO_2), nitric oxide (NO) and sulfur dioxide (SO_2). Particle and moisture filters were used upstream of the gas analyzer to inhibit the entrance of moisture and soot into the gas analyzer. 5 cm further downstream from the sampling probes employed for gaseous species, a humidity sensor (Omega, Model RH-USB) was also used to measure the relative humidity in the exhaust hood.

The gaseous species concentrations and temperatures were obtained using two separate data acquisition cards connected to a National Instruments LabView program where each of the data sets were acquired at a frequency of 10 Hz. A calibration gas with a composition of 10% CO_2, 1% CO, and 21% O_2, as well as one with 5000 ppm of NO and SO_2 were utilized to provide calibrations for the gas analyzer. Two Alicat flow controllers were used to vary the concentrations of calibration gases to ensure a multiple point calibration, improving the accuracy of the calibration process. Nitrogen (N_2) gas was passed through the gas analyzer before the calibration process to provide zero concentrations for each gas column and to eliminate any residual gases in the lines. Fig. 4 shows the calibration curve of CO_2. It is found that when the concentration of CO_2 is below 0.4% which is also the range of our experimental measurements, the calibration curve is not linear. Furthermore, an air baseline was also measured before each experiment where the values of CO_2 and CO in the air were deducted from the measurements. The particulate analyzer used in this study was calibrated by the manufacturer (TSI) against Arizona Test Dust (ISO 12103-1) for $PM_{2.5}$ measurements and before each set of experiments, the DustTrak was zeroed using the device's internal auto-zero function and a 0 PM filter before each experiment. A nominal flow rate of 2 SLPM was specified for flow into the DustTrak via its internal pump system.

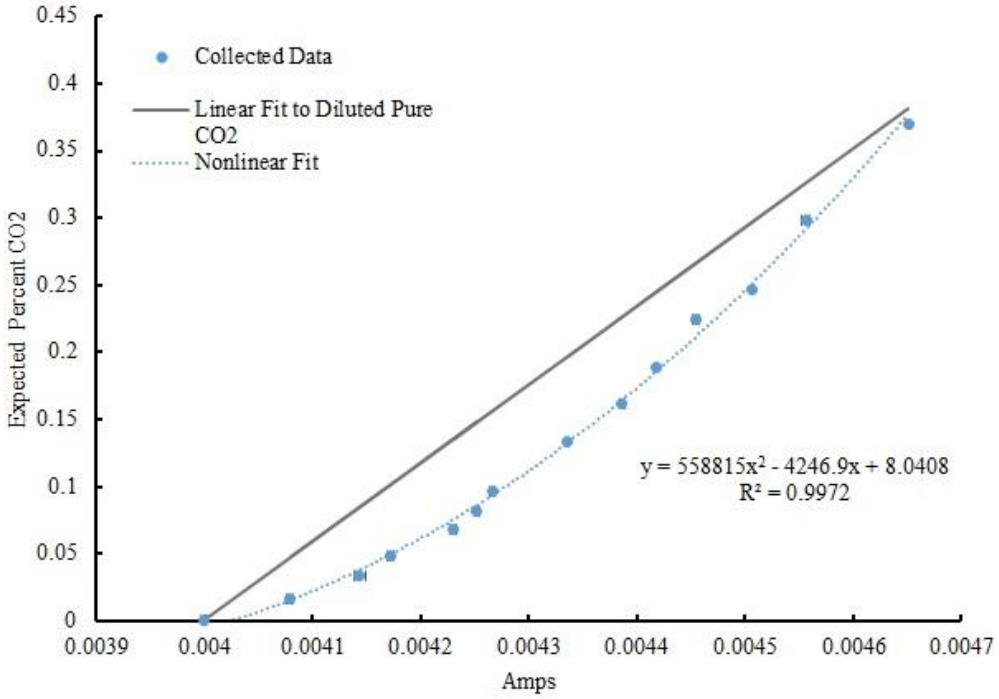

Fig. 4 Calibration curve for ZPA CO_2 measurement
Nonlinear calibration curve for ZPA CO_2 measurement when the concentration is below 0.4%. The linear calibration curve when the concentration is above 0.4% is added for comparison.

3 Phase I: Fire Whirl Design

3.1 Task I: Prototype Design

Phase I, Task I of this project was designed to test various configurations for a fire whirl generator at a small scale. From these tests, the effects on burning characteristics and fire whirl geometry for each configuration was analyzed for trends with configuration parameters.

An investigation was carried out into the effect of the height of the enclosure over the pool surface. Ideally, the shortest wall height that maximizes the fire whirl's benefits of increased burning rate and reduced emissions will be selected so that it is as easy as possible to deploy in an open-ocean configuration. A four-walled enclosure following previous work was used for this series of experiments. The fuel used in these experiments was a 2.5 mm thick slick of n-heptane in a 10 cm diameter pool over a water layer. For effective wall heights, H = 5 cm to H = 55 cm, the burning rate and flame length were recorded. The mass loss rate was calculated as the difference between instantaneous mass measurements at a rate of 1.75 Hz, with the average mass loss rate taken as the average of these differences during the period of steady burning. These results are shown in Fig. 5. The flame height was captured by recording the burning duration and measuring the pixel length of the pixels above a threshold brightness for each frame over the steady burning period. The flame heights are shown in Fig. 6.

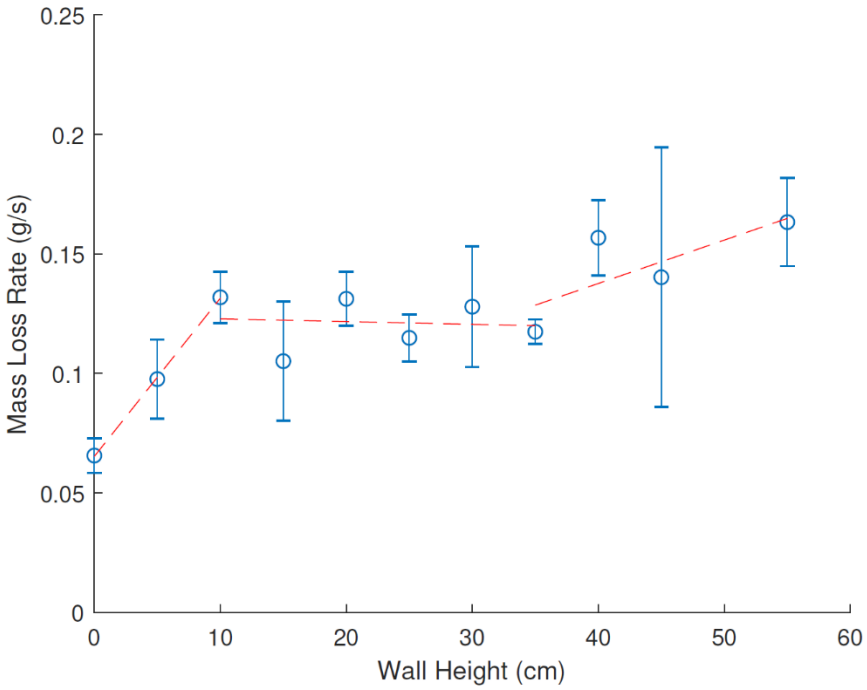

Fig. 5 Mass loss rate with different enclosure height
Mass loss rate for enclosure heights H=0 to H=55 cm, and a pool diameter of D_0=10 cm. Points show averaged values with error bars representing the standard deviation between test averages during each test's steady burning period.

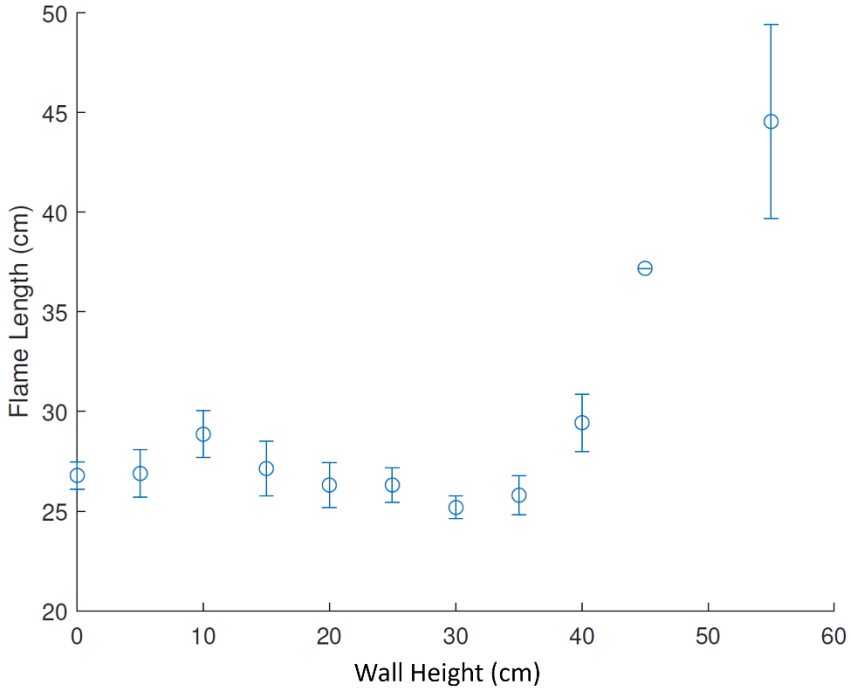

Fig. 6 Flame length with different enclosure height
Flame length in cm for enclosure heights H=0 to H=55 cm with a pool diameter of D_0=10 cm. Points show averaged values with error bars representing the standard deviation between test averages during each test's steady burning period.

From these figures, it is noted that there was a substantial increase in mass loss rate when compared to a pool fire for walls with an effective height as low as H = 10 cm while there was no great increase in flame length until H = 30 cm. Additionally, captured video allowed for a quantification of the fire whirl stability represented by the tilt of the flame tip away from perpendicular to the fuel surface, shown in Fig. 7. This showed two critical values, one at H = 10 cm when the effects of the enclosure began to influence the behavior of the flame, and one at H = 35 cm beyond which the flame became a stable fire whirl rather than an unstable precessing flame.

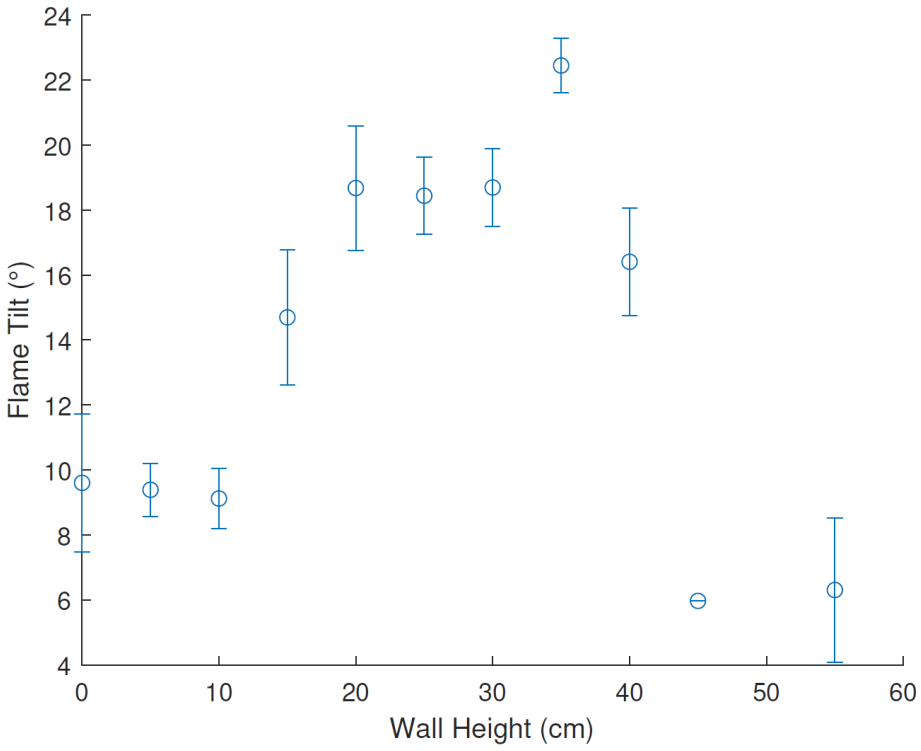

Fig. 7 Flame tilt with different enclosure height
Degree of inclination of the flame tip for enclosure heights H=0 to H=55 cm with a pool diameter of D_0=10 cm. Points show averaged values with error bars representing the standard deviation between test averages during each test's steady burning period.

These preliminary experiments revealed that the addition of tangential flow entrainment via the introduction of walls and gaps appeared to enhance the burning rate of a fuel pool long before the formation of a traditional fire whirl. The fact that the burning rate nearly doubles for wall heights on the order of the pool diameter present a potential opportunity for low wall heights may not form traditional, vortex-like fire whirls, but may vitiate combustion sufficiently to achieve the desired step-change in efficiency and effectiveness of in-situ burning. Additional enhancement in burning rate was still observed once the flame lengthens into a traditional fire whirl, at wall heights between 4-6 times the fuel pool diameter, however if desired outcomes are achieved without reaching this height a suitable solution may be able to use lower wall heights. The fire whirl may be less stable within these intermediary wall heights, rotating and filling much of the test apparatus, however this may be permissible depending on the final design chosen and will be studied further. One notable absence in this series of testing is emissions testing which will be incorporated later.

A second series of experiments were carried out to determine the limits of fire whirl formation for these low wall heights. These tests were conducted using a three-wall configuration with a wall height of H = 12 cm. The three-wall configuration was chosen because (1) it was found to produce very stable fire whirls in earlier testing, (2) it presents a simplified setup with one less piece, (3) geometrically it is superior offering less regions of recirculation and a smoother flow within the apparatus, and (4) it may coincide with a shape that can more easily be towed behind

boats and sectioned together over an in-situ burn. The configuration used in the laboratory is shown in Fig. 8. These tests had no water layer under the n-heptane and instead used a 5 mm thick pool, simplifying testing without affecting results considerably. Notably, the pool fire tested in this way had a burning rate higher than that shown in Fig. 5.The results of these tests are shown in Table 2, where D_c represents the distance from the center of the fuel pool to the wall rather than the pool diameter, and G represents the width of the inlet gap. For the smaller enclosures, a definite increase is shown in mass loss rate compared with three walls and gaps compared to a pool fire of the same size. For the larger enclosures, with more separation between the fuel pool (fixed at D_0 = 10 cm) the flame behaved as a pool fire with a similar burning rate regardless of the gap size. One data point of note here is the very high mass loss rate for the smallest enclosure. These flames did not produce a strong fire whirl but did show a marked increase in mass loss rate compared to the other flames in this series of tests, beginning to show transient vortex structures in the flame. The flame itself was much larger than the pool or other experiments with larger enclosure sizes. This is likely due, at least in part, to the increased heat feedback from the aluminum walls of the enclosure and represents another parameter to optimize in testing at increasing scales. The flame also visibly touched the walls as shown in Fig. 9. This may be a concern for future tests where the size of the fuel pool is large compared to the area of the enclosure floor unless the apparatus is made to withstand this significant heating. Further tests were performed with walls of heights H = 30 cm and H = 35 cm to form a strong fire whirl with both increased mass loss rates and increased flame heights. These configurations are tested in phase II with the exhaust sampling system to define improvement/detriment in emissions.

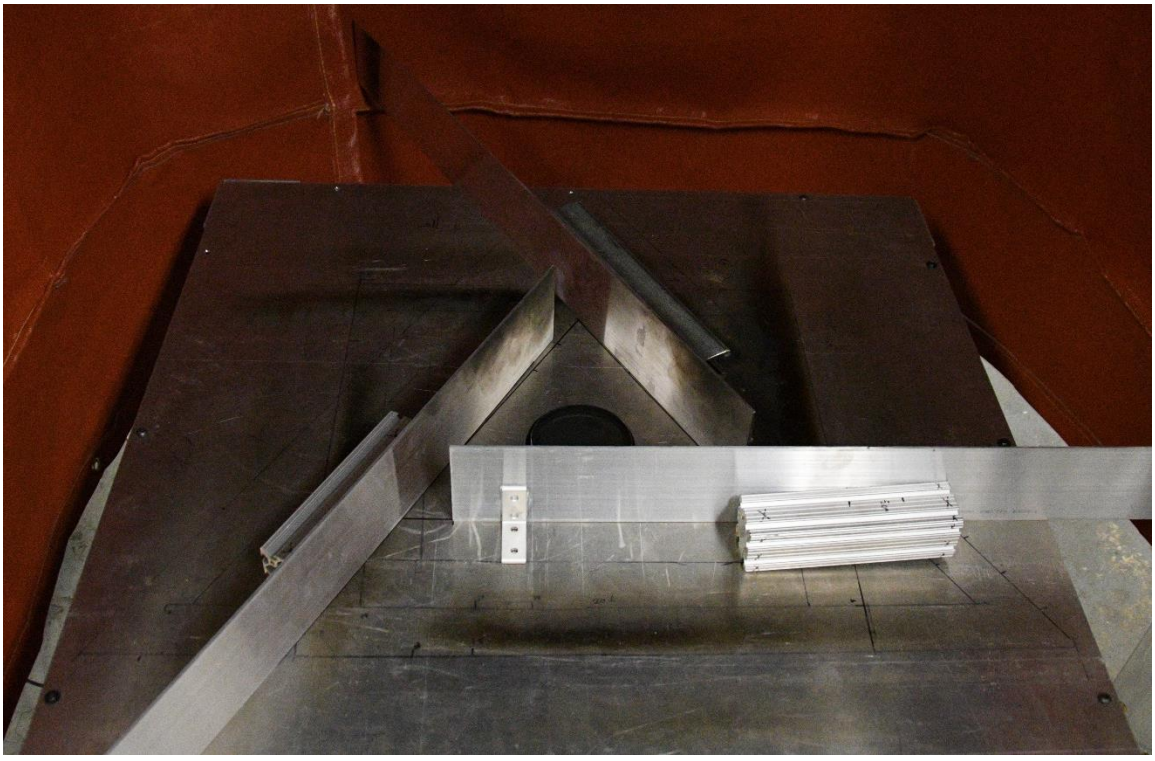

Fig. 8 Photo of three-wall enclosure
Three-wall enclosure with a wall height H = 10 cm, with a distance D_c = 10 cm between the center of the pool and the wall, and a gap size G = 5 cm.

Table 2 Mass loss rates for varied enclosure diameter D_c and gap size G with a fixed wall height of 10 cm.		
D_c (cm)	**G = 5 cm**	**G = 10 cm**
10	0.1487 g/s	0.1505 g/s
15	0.1141 g/s	0.1161 g/s
20	0.0983 g/s	0.1070 g/s
Pool fire	0.0975 g/s	

Fig. 9 Photo of flame touching the walls
Large flame touching the enclosure walls and demonstrating transient fire whirl formation for an enclosure D_c = 10 cm, H = 10 cm.

3.2 Task II: Prototype Emissions Measurements

The goals of Phase I Task II are to provide emissions measurements for fire whirls generated via the designs explored in Phase I Task I. From these, trends in species and particulate matter emissions for varying design parameters are to be established. These trends, combined with the mass loss rate and flame geometry results from Task I are to inform the creation of a prototype configuration at the small to medium scale. A series of experiments were performed to quantify emissions from a fire whirl with a three-wall enclosure. Experiments were designed based on preliminary results using a three-wall structure for the formation of fire whirls with varying wall height and gap size, where the objective was to choose the set of conditions at each wall height with the highest burning rates based on the previous experiments. In this regard, three sets of conditions were chosen which are summarized in Table 3. The first set of experiments were

using “tall walls”, second with “short walls” and the third one representing the conditions of a pool fire (no wall). Fig. 10 shows photos taken during these experiments. Preliminary experiments were performed using these conditions where the measured data included the generation of $PM_{2.5}$, mass loss rate, average temperature, and masses of generated gases.

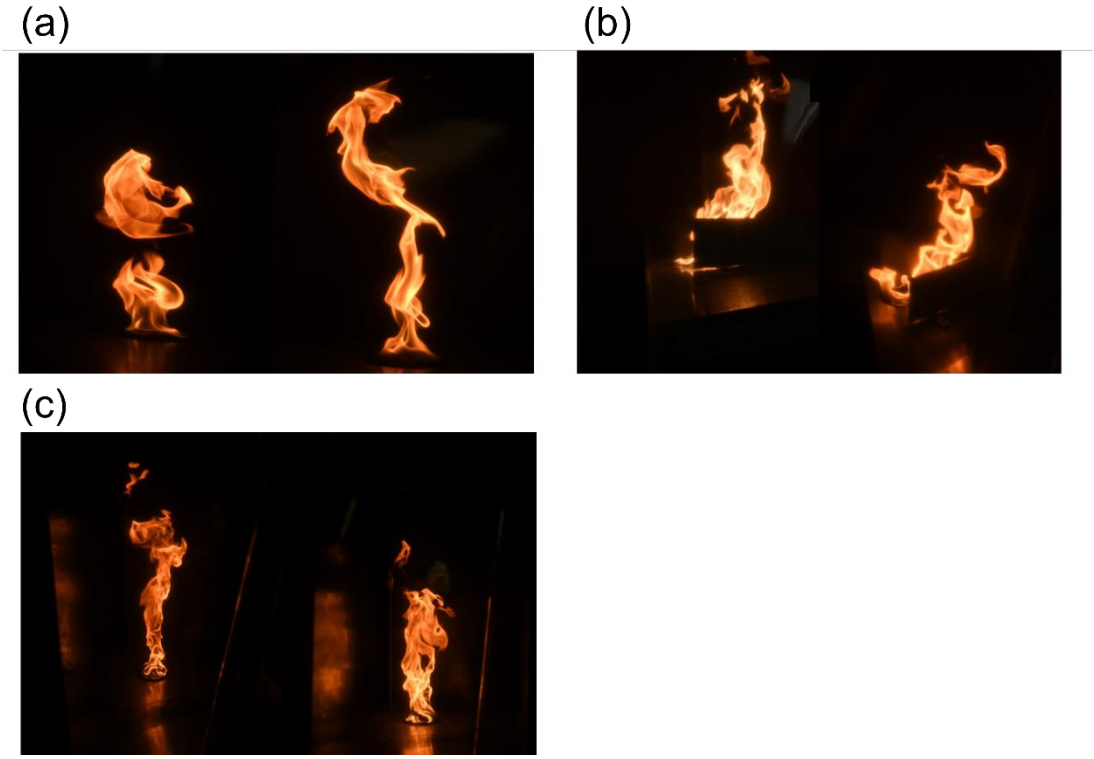

Fig. 10 Photos of fire whirls with different wall height
Images of the flame produced in (a) a pool fire, (b) the short-wall fire whirl generator and (c) the tall-wall fire whirl generator.

Table 3 Experimental conditions in prototyping

Experiment type	H (cm)	D_c (cm)	G (cm)	D_0 (cm)
Fire whirl with tall walls	60	15	10	10
Fire whirl with short walls	12	10	10	10
Pool fire	-	-	-	10

Fig. 11 demonstrates the average variation of mass over time for the three sets of conditions as mentioned in Table 3, where the initial mass of heptane fuel for each experiment was 20 g. It can be observed that, on average, a fire whirl structure with a tall wall height resulted in burning the fuel in a shorter duration of time as compared to a fire whirl with a short wall, and a pool fire. The slope of this figure can be used to estimate the mass loss rate for each condition, where for the tall wall, short wall and the pool fire, the average mass loss rate was observed to be 0.184 ± 0.011 g/s, 0.119 ± 0.020 g/s and 0.094 ± 0.012 g/s, respectively. The uncertainty in each test was calculated using the student t-test method.

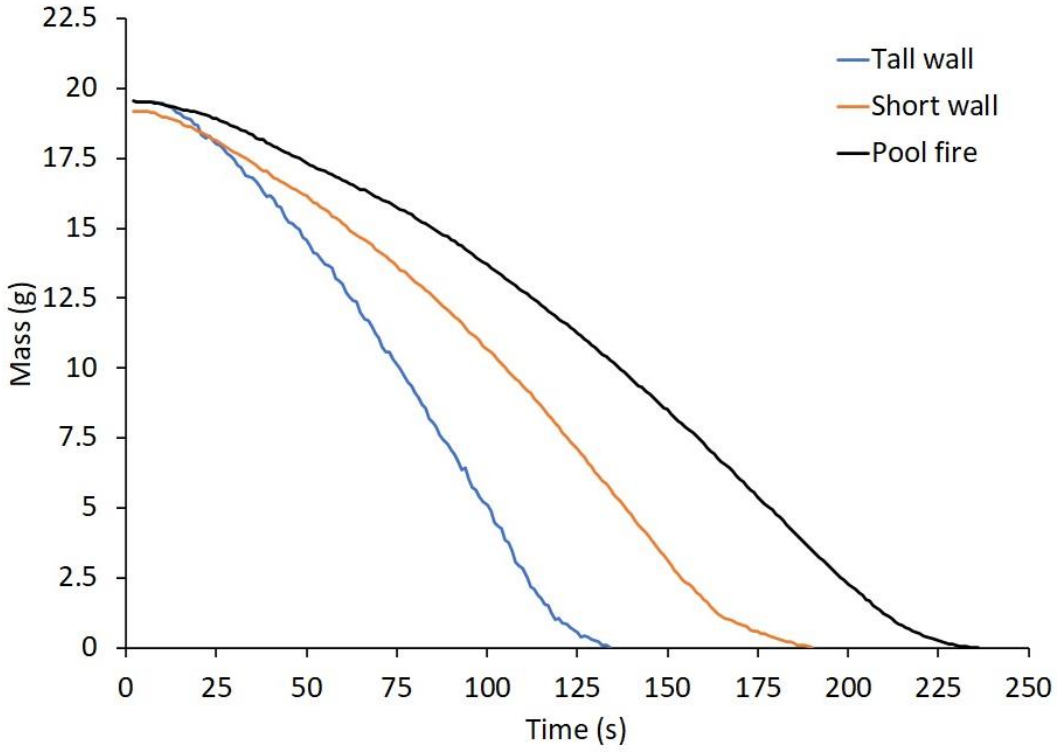

Fig. 11 Mass loss vs time
Average instantaneous mass for each generator configuration shown as a function of time since ignition.

Fig. 12 shows the averaged mass loss rate profiles for the three conditions. Mass loss rate was defined as the derivative of mass in increments of one second. It should be noted that the cut-off time in this figure and for each condition was when the experimentation or data logging were stopped, and in some cases negative masses were seen in the mass balance at the end of the experiments, which warrants further investigation and will be addressed in future updates. The significance of this plot is that when multiplied by the heat of combustion, heat release rate profiles of each experiment can be obtained. Based on this figure, it can be observed that the burning rate of a generated fire whirl with a tall wall height configuration were higher than the one with a short wall height and the pool fire, respectively. Moreover, Fig. 13 shows the measurements of $PM_{2.5}$ for the three sets of experimental conditions with the tall and short wall fire whirls as well as the pool fire. The data were plotted using a 10-point moving average formula for all experiments. It can be seen that the highest amount of particulate matter generation was observed in the fire whirl configuration with a short wall height compared to the one with taller height and the pool fire, respectively. The average mass of generated particulates for a tall wall fire whirl configuration, short wall fire whirl configuration as well as the pool fire were seen to be 212.6 ± 1.3 mg, 428.6 ± 17 mg and 410.6 ± 18.1 mg respectively, with errors calculated using the student t-test method with 95% confidence interval. Overall, it was observed that the tall wall fire whirl had the highest burning rate and the lowest amount of particulate matter. These results were based on a number of limited experiments and warrant further investigation.

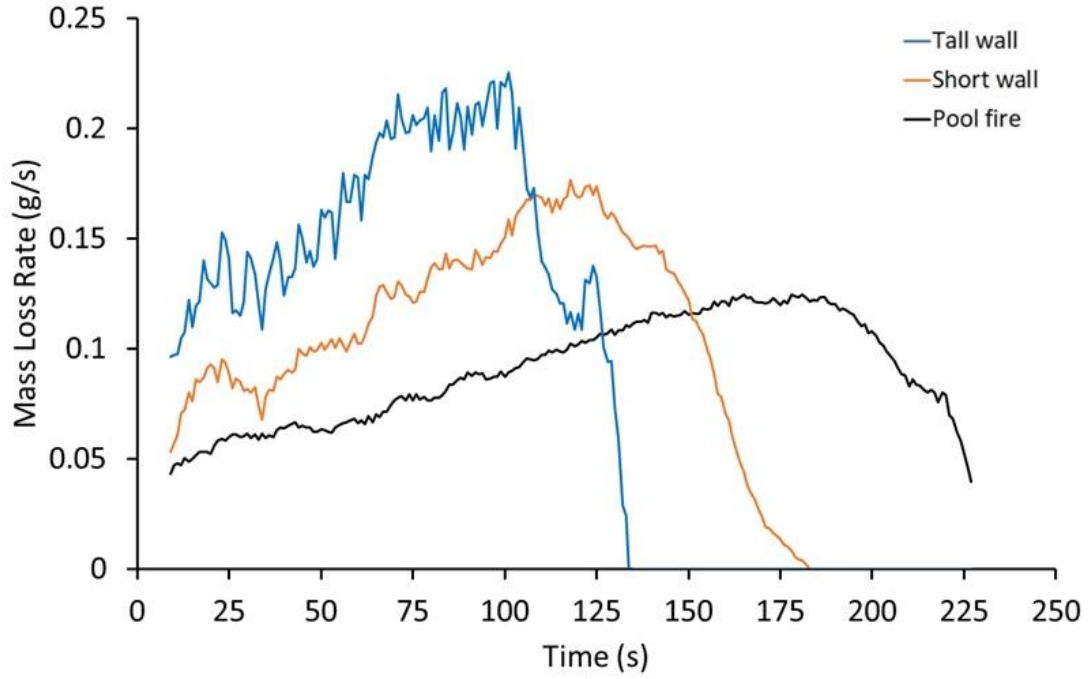

Fig. 12 Mass loss rate vs time
Mass loss rate as a function of time for the three sets of experimental conditions.

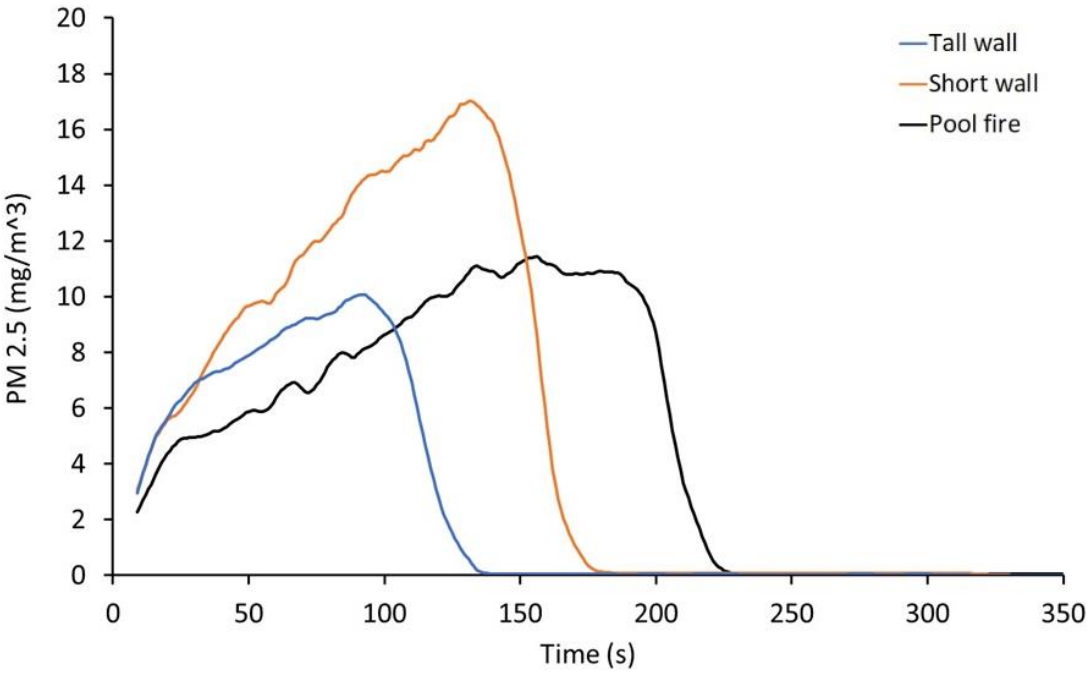

Fig. 13 Emission concentration of $PM_{2.5}$ vs time
$PM_{2.5}$ generation profiles as function of time for the three sets of experimental conditions.

Sample measurements from gaseous product species as well as the generation rate profiles of CO_2 and CO are shown in Fig. 14 and Fig. 15. These results correspond to a test for a fire whirl with a short wall height enclosure. As mentioned earlier, measurements of the average temperature profile as well as the concentrations of CO_2, CO and O_2 were performed. Using these data, mass generation profiles were also obtained where the area under the curve could be utilized to calculate the mass of generated species. Experiments were performed for the fire whirl with tall walls, short walls and the pool fire and it observed that CO_2 production for these conditions were 64.0 ± 19.0 g, 64.33 ± 9.9 g, and 65.0 ± 16.23 g, respectively, with the uncertainties calculated using the student t-test method with 95% confidence interval. The initial results point towards the feasibility of the system to measure different gas concentrations. It was also observed in the experiments that the CO emissions were negligible in all the tests. These results, however, are preliminary and limited, and more experiments are required to confirm the observed trends along with quantification of their uncertainty.

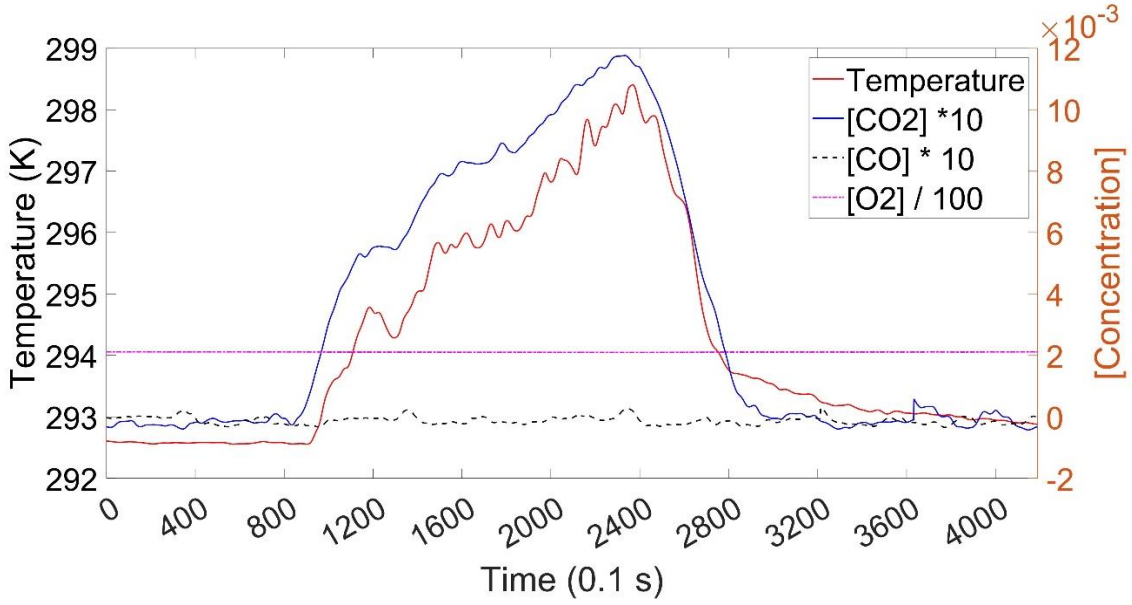

Fig. 14 Emission concentration of gases vs time
Average temperature, and gaseous species concentration profiles for a fire whirl test with a short wall height.

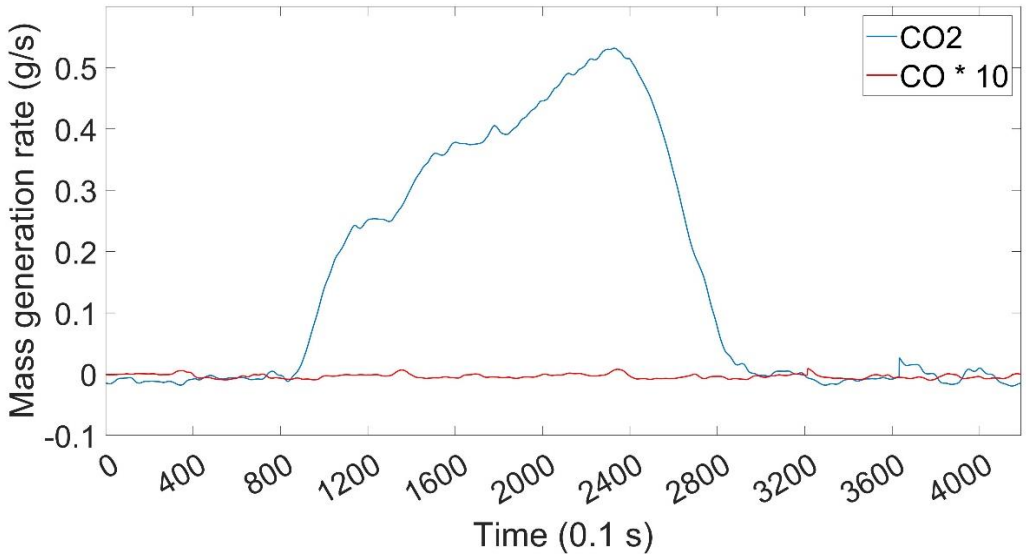

Fig. 15 Mass generation rate of gases vs time
Mass generation rate profiles of CO_2 and CO for a fire whirl test with a short wall height.

Additionally, Fig. 16 shows a comparison between the average mass generate rate profiles of CO_2 for the fire whirl with a tall wall height, short wall height, and the pool fire. These can be interpreted as proportional to the heat release rate of the fire. It can be seen that on average the highest peak for the mass generation of CO_2 corresponds to the fire whirl with a short wall height, followed by the fire whirl with a tall wall height, and the pool fire.

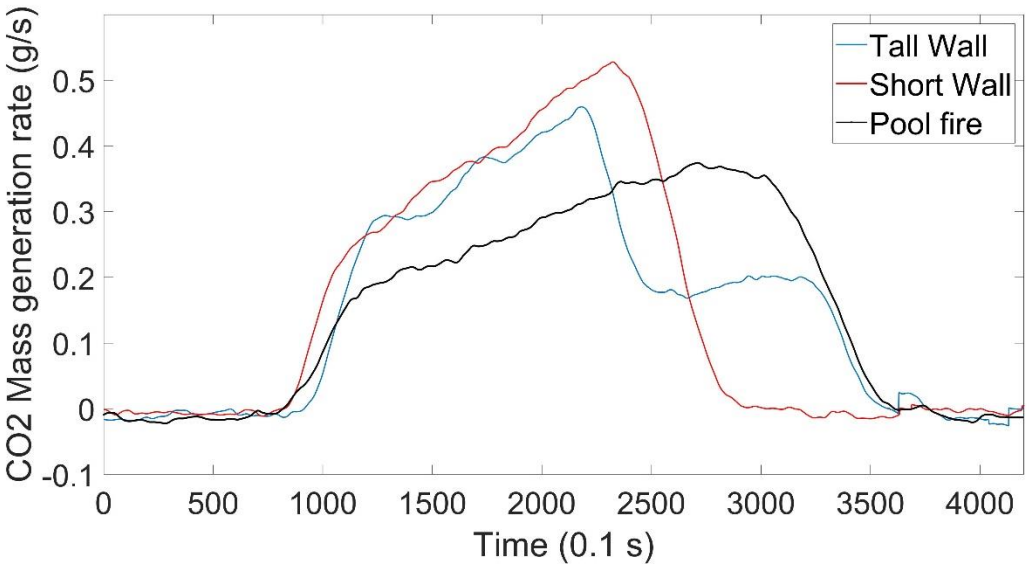

Fig. 16 Mass generation rate of CO_2 vs time
Comparison between the average mass generation rate profiles of CO_2 for a fire whirl test with a tall wall height, short wall height, and the pool fire.

3.3 Final Prototype Selection

Based on the emissions measurements from Task II and the burning (mass loss) rates established in Task I and repeated in Task II, the recommendation for a prototype at the small and medium scale has been selected as a three-wall tall fire whirl generator. The advantage of this setup over the four-wall setup is additional simplicity in a static design and good stability of the structure. Based on results of tests the gap between the walls should be approximately 20% of the side length of the triangle. Fig. 17 shows a photograph of the tall-wall fire whirl prototype selected.

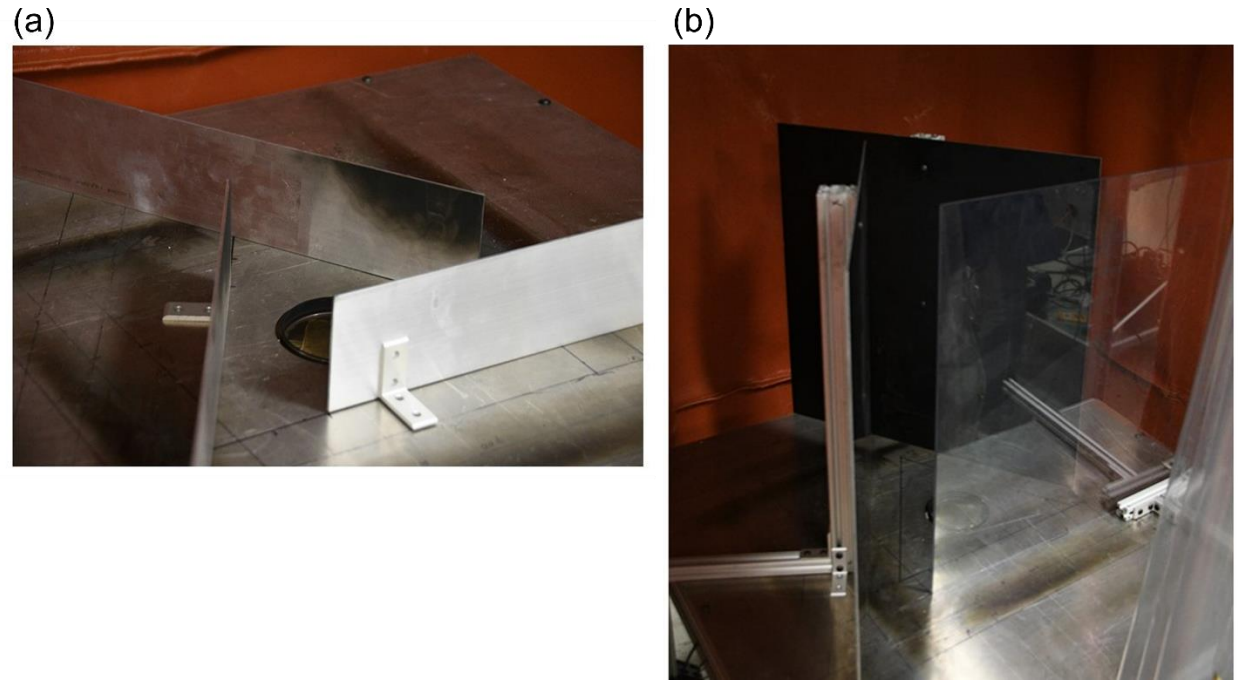

Fig. 17 Photos of fire whirl prototype
Photographs showing (a) the short-wall and (b) the tall-wall fire whirl enclosures.

The ideal wall height of the setup was a point of particular interest as lower wall heights would provide an advantage in stability, ease of deployment, etc. four-wall structure results saw the greatest mass loss rates with the tallest wall height (see Figure Fig. 5); however, there was still a significant improvement in burning rate at the small wall height without adding the significant extra material necessary for the tall wall. There still was an improvement in burning rates for the small height but it was not as dramatic of an improvement as in the four-wall setups. This improved burning rate, however, did not translate to $PM_{2.5}$ emissions, which were actually highest for the short wall setup, with the no-wall pool fire in the middle, and the lowest (cleanest burning) for the tall wall setup.

Because of the reduced emissions and highest burning rates achieved, the tall wall is still the ideal setup of choice. Higher burning rates also indicate higher heat fluxes to the fuel surface which, in previous results from the first BSEE fire whirl study, resulted in increased amounts of crude oil burned at small scales. This could be beneficial to study if fire whirls could improve the effectiveness of burning residue in more challenging scenarios, such as with emulsified oil.

As this investigation continued into Phase II, emissions measurements and burning efficiency of crude oil with varied slick thicknesses were all investigated on this tall-wall setup. A more detailed investigation of wall height is proposed in the future to ensure we have reached an optimum height and to better understand the mechanism of emissions reduction with taller walls but was not completed as it was out of scope of this contract. This future work may inform why the short wall generator produces fire whirls with comparable $PM_{2.5}$ emissions to a pool fire, but this may improve as the burn duration increases with greater slick thicknesses.

4 Phase II: Effect of Slick Thickness on Emissions and Efficiency

Phase II studied the effect of slick thickness on burning efficiency and emissions with and without a fire whirl burning two types of crude oil (HOOPS and ANS) for different slick thickness in experimental conditions of pool fire and fire whirls. Key findings include the fuel consumption efficiency and emission factors of particulate matter (PM). Work completed in Phase II also was essential to prepare for large-scale prototype experiments in Phase III.

4.1 Experimental Methodology

The objectives of Phase II Task 1 are to identify trends of emissions, residual weight, consumption efficiency etc. with slick thickness. This includes the various species emitted (e.g., CO_2, CO, SO_2, NO_X, PM) to attempt to capture an overall mass balance. Changes in slick thickness that provides best estimates for long-term steady-state burning were also conducted, which can then be used for actual predictions of emissions reductions in ISBs. Experiments were performed for both pool fires and fire whirls. Results are compared between different crude oils.

Phase II Task 2 includes data assimilation and dissemination, interpreting and analyzing results from Phase II, Task 1. Analysis of ANS and HOOPS data for different slick thicknesses including fuel consumption efficiency, emissions, flame height, and temperature in the pool will be conducted. The results are being prepared for publication and comparison to Phase III experiments.

The experimental setup was introduced earlier. The fire whirl apparatus was constructed by using a three-wall structure and placed over a 10 cm diameter pool. The results were compared to a pool fire with the same diameter fuel pool. The fire whirl enclosure formed an equilateral triangle with a single gap G = 10 cm on each side wall to allow for the tangential entrainment of air. The height of the walls is H = 60 cm matching the height from Phase I that showed peaks in mass loss rate for a four-wall enclosure. The walls were used to form an enclosure with a side length S = 52 cm. Each experiment used nominal volumes of 30 ml, 60 ml, and 90 ml of crude oil as fuel to form the fire whirl.

4.2 Results of Fuel Consumption Efficiency and Emissions

In this study, the effect of fuel slick thickness on the emissions as well as the mass loss rate were investigated by using both HOOPS and ANS crude oil where the difference in slick thickness was achieved by adding different volume of fuel (30 ml, 60 ml, and 90 ml), with the fuel pool having a diameter of 10 cm. In each experiment, the fuel was poured over a water layer to represent the conditions analogous to an oil spill over open water. The two types of in-situ burning experiments using pool fires as well as fire whirls were performed to compare the mass loss rate as well as the emissions between the two methods. At least five experiments were performed at each condition and error bars are shown in the subsequent plots to represent deviations between averages between repeated experiments. Note that most results presented here are for the pre-boilover stage, as the boilover stage is often short, disrupts mass

measurement techniques, and may not be representative of full-scale behavior where boilover is not commonly observed. Fig. 18 shows the mass loss progress of six experiments using ANS in different slick thickness by using 30, 60, and 90 ml fuel for fire whirl and pool fire tests. In the figure, boilover happens at the change of mass loss rate near the end of burning and the interruptions of data were caused by boilover.

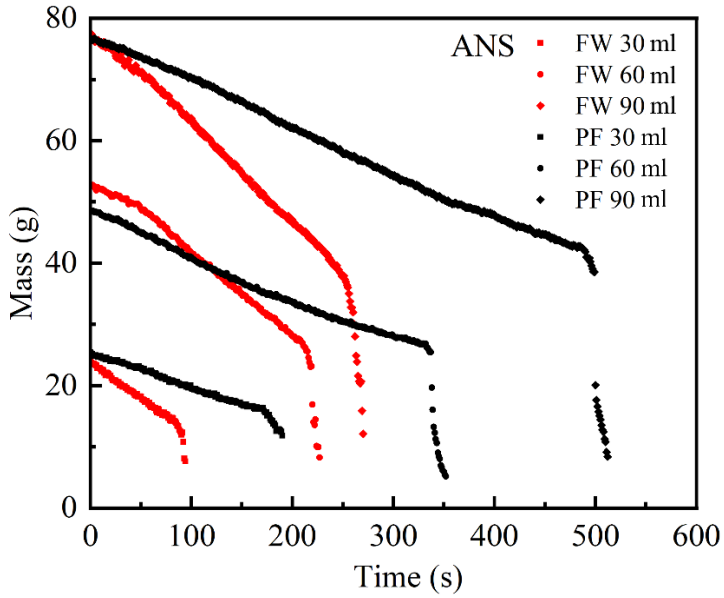

Fig. 18 Mass loss with time
Mass loss progress of fire whirl and pool fire burning ANS in different slick thickness. The change of mass loss rate and interruption in data points were caused by boilover.

The comparisons of burning rates for all experiments at pre-boilover stage are shown in Fig. 19. At all fuel thicknesses, the fire whirl showed a higher burning rate than the pool fire configuration. Additionally, the burning rate is shown to increase with increasing slick thickness for both the ANS and HOOPS fire whirls, while pool fires have much lower variations in burning rates by changing the slick thickness.

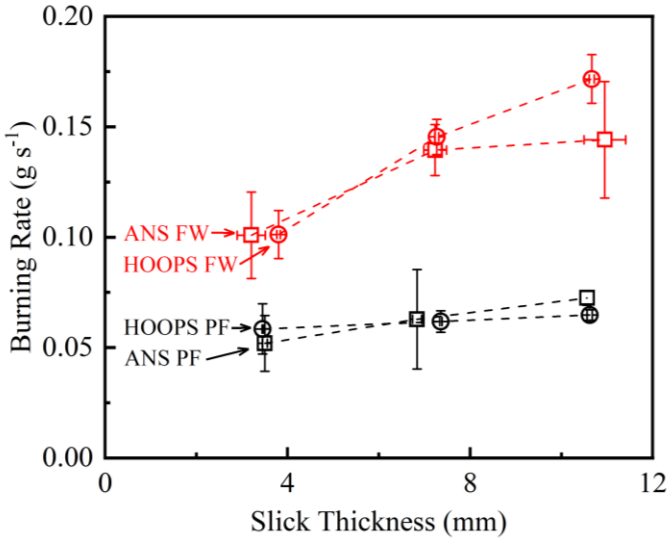

Fig. 19 Burning rate with slick thickness
Comparison of burning rate (pre-boilover) in this study for HOOPS and ANS in different slick thickness.

The starting mass of the fuel and the remaining mass after the burning process were also recorded for each experiment. Fuel consumption efficiency is calculated as the ratio of mass loss in the burning process, including boilover, to the total initial mass of the fuel. Fig. 20 shows the comparisons of the fuel consumption efficiency for all cases in this study. For both HOOPS and ANS, increasing slick thickness results in an increase of fuel consumption efficiency. In all cases, the fire whirl configuration has a higher fuel consumption efficiency than the pool fire configuration.

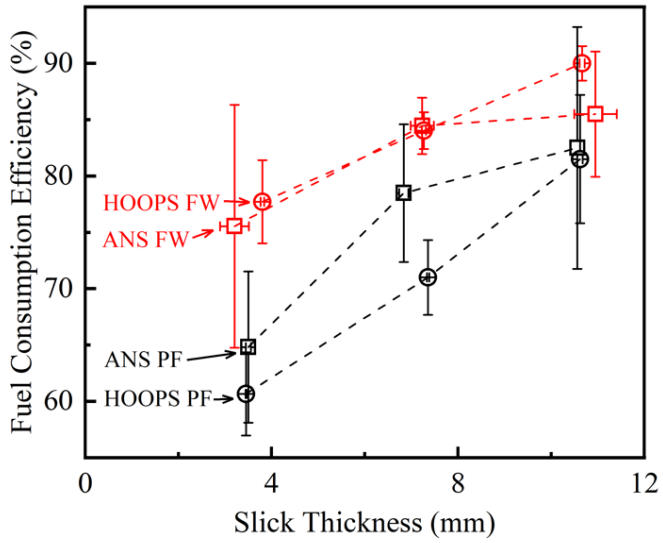

Fig. 20 Fuel consumption efficiency with slick thickness
Fuel consumption efficiency for HOOPS and ANS by varying slick thickness.

By increasing the slick thickness, the steady burning duration increases as well. Fig. 21 shows the steady burning duration for all experimental conditions. Pool fires nearly doubled the burning duration compared to fire whirls. Thermal penetration rate, calculated by tracking the temperature increase in thermocouples in the oil layer and the oil-water interface, do not show a significant trend when increasing the slick thickness, shown in Fig. 22. In ANS experiments, thermal penetration rate is higher in fire whirls than pool fires, while in HOOPS experiments, thermal penetration rate does not have a significant difference between fire whirls and pool fires. The thermal penetration rate in ANS is higher than in HOOPS.

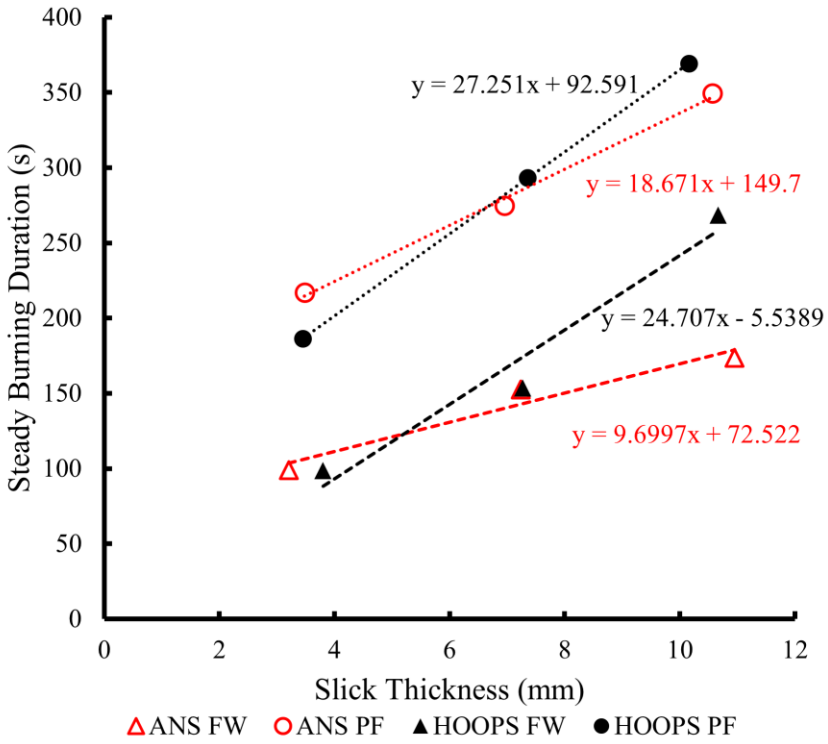

Fig. 21 Steady burning duration with slick thickness
The steady burning duration for HOOPS and ANS with different slick thickness in fire whirl and pool fire experiments.

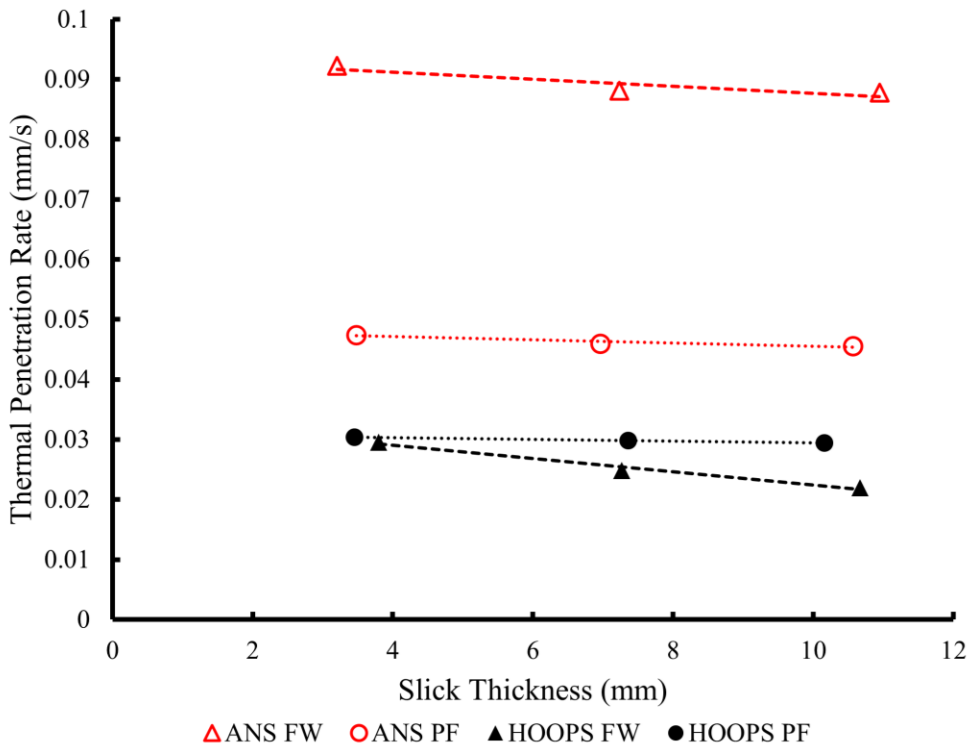

Fig. 22 Thermal penetration rate with slick thickness
The thermal penetration rate for HOOPS and ANS with different slick thickness in fire whirl and pool fire experiments.

The heat release rate (HRR) in this experiment was calculated by using the method of oxygen consumption calorimetry. This was done by multiplying the oxygen concentrations by a constant value of 13,100 MJ/kg of O_2, which is the constant amount of heat that is released per unit mass of oxygen consumed (assume complete combustion). A reduction in the oxygen percentage was measured using the oxygen sensor of ZPA, which was then converted to HRR. The averaged HRR at the steady stage of burning for all experiments are summarized in Fig. 23. The averaged HRR at the steady stage is higher in fire whirls compared to pool fires. The steady stage HRR increases with the increase of slick thickness. As there is a significant jump in HRR at the onset of boilover, the boilover intensity is calculated as the peak HRR over the averaged HRR at steady stage, shown in Fig. 24. The results show pool fires have higher boilover intensity than fire whirls and by increasing slick thickness, boilover intensity has a trend of increasing.

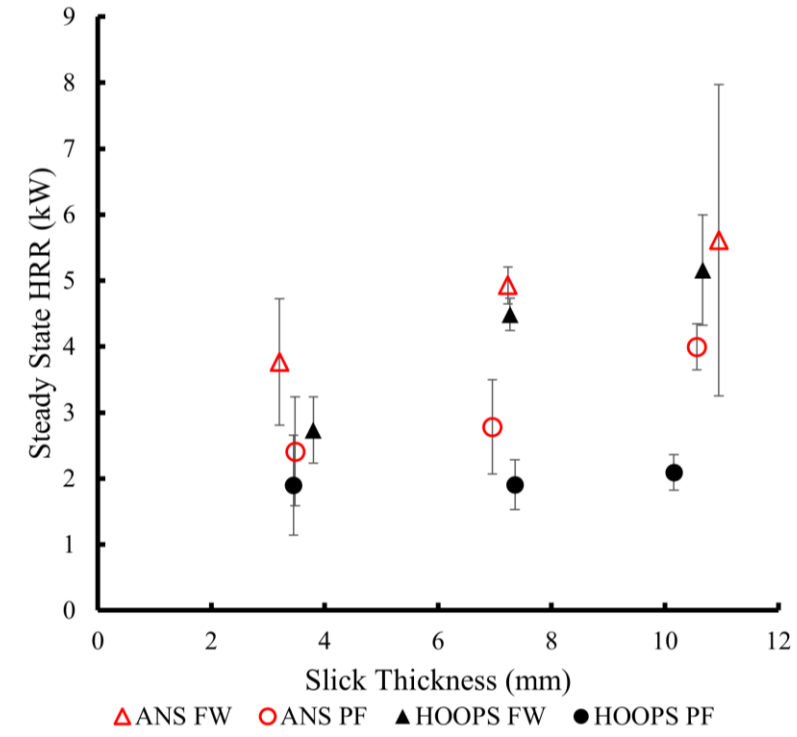

Fig. 23 Steady state HRR with slick thickness
Steady state HRR for HOOPS and ANS with different slick thickness in fire whirl and pool fire experiments.

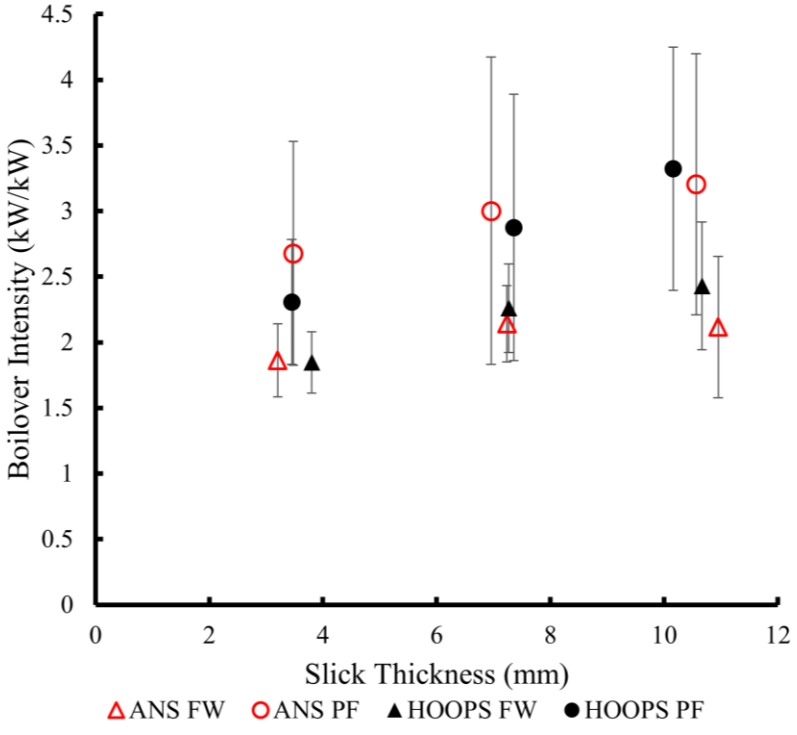

Fig. 24 Boilover intensity with slick thickness
Boilover intensity for HOOPS and ANS with different slick thickness in fire whirl and pool fire experiments.

Fig. 25**Error! Reference source not found.** and Fig. 26**Error! Reference source not found.** show the emission factors of CO_2 and CO. From the results, in experiments using ANS, pool fires have higher emission factors of CO_2 than fire whirls, while in experiments using HOOPS, there is no significant difference between the results of pool fires and fire whirls. There is no significant difference between fire whirls and pool fires in the results of CO emission factors. By increasing the slick thickness, the emission factors of CO_2 and CO do not have a clear trend in changing, with emission factor of CO_2 in the range of 2.6 – 3.0 g/kg, and emission factor of CO in the range of 0.01 – 0.04 g/kg. Fig. 27**Error! Reference source not found.** shows the results of modified combustion efficiency (MCE) at steady stage which is calculated as the concentration of CO_2 over the sum of the concentrations of CO_2 and CO. The MCE for all experiments is in the range of 0.97 – 0.99.

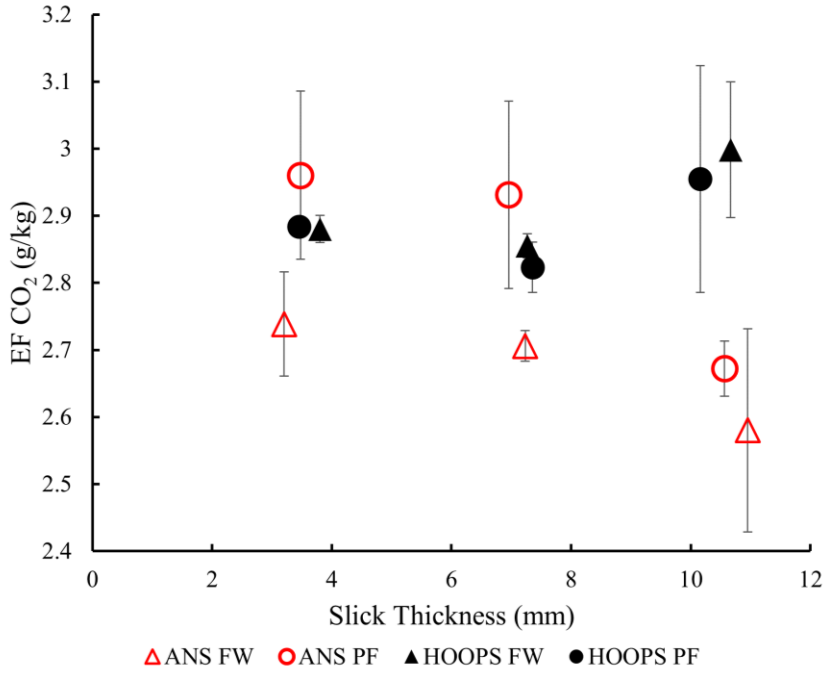

Fig. 25 EF CO_2 with slick thickness
EF CO_2 for HOOPS and ANS with different slick thickness in fire whirl and pool fire experiments.

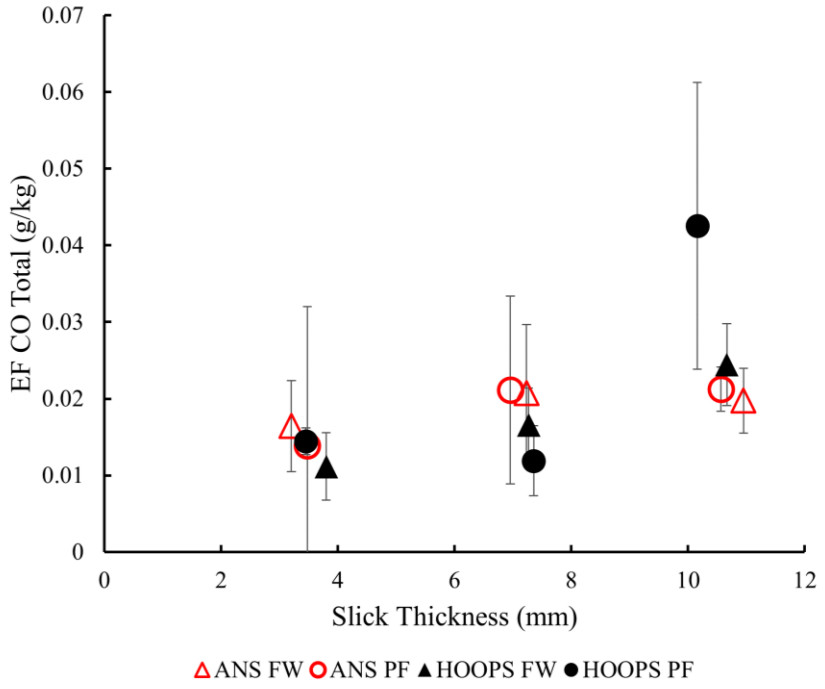

Fig. 26 EF CO with slick thickness
EF CO for HOOPS and ANS with different slick thickness in fire whirl and pool fire experiments.

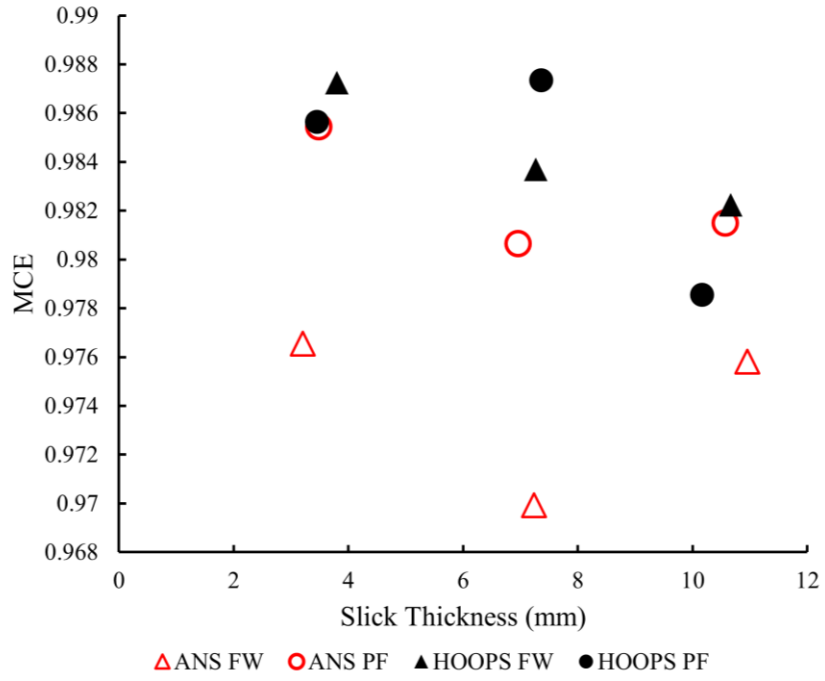

Fig. 27 MCE with slick thickness
MCE for HOOPS and ANS with different slick thickness in fire whirl and pool fire experiments.

The emissions factor of $PM_{2.5}$ was calculated as the average mass of particulate matter produced before boilover divided by the mass of crude oil burned before boilover, and is shown in Fig. 28. For all slick thicknesses, the fire whirl had a lower EF $PM_{2.5}$, although both conditions showed a slight increase in $PM_{2.5}$ production with slick thickness. Comparing the results of different fuels, ANS has higher emission factors of PM than HOOPS. Fig. 29**Error! Reference source not found.** shows that there is a positive correlation between the emission factor of $PM_{2.5}$ and surface mass flux.

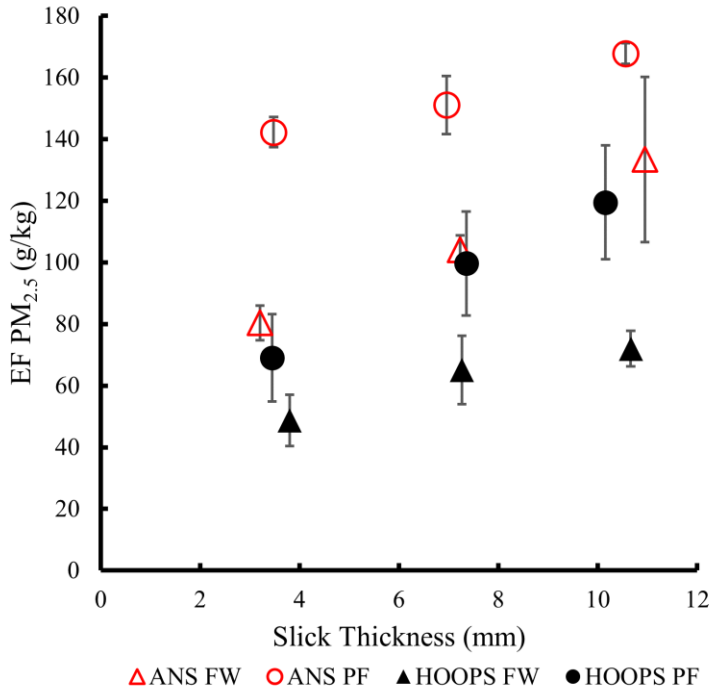

Fig. 28 EF PM with slick thickness
Comparison of EF PM for HOOPS and ANS at varying slick thickness. Note this includes data pre-boilover only.

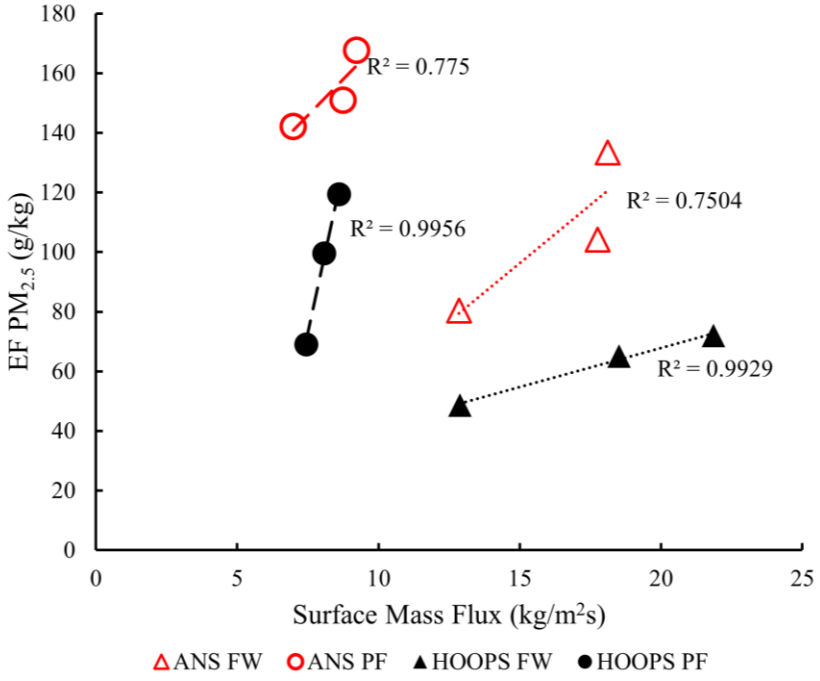

Fig. 29 EF PM with surface mass flux
Comparison of EF PM for HOOPS and ANS at different surface mass flux by varying slick thickness. Note this includes data pre-boilover only.

5 Phase III: Large-Scale Fire Whirl Demonstration

5.1 Experiment Objectives and Overview

For Phase III large-scale fire whirl experiments were successfully conducted at the proposed testing site, the TEEX Brayton Fire Training Field in College Station, Texas during May 15-19, 2023. All parties in this BSEE project, including participants from BSEE, UCB, TAMU, USGS and EPA, and TEEX, worked hard and cooperated to safely conduct these experiments (Fig. 30 is a photo of most of the participants in this project at the testing site). This chapter reviews the experimental setups used and presents the results from this experiment.

Fig. 30 Group photo
Group photo of most of the participants in the large-scale experiment at the testing site. (Photo: USGS, 2023)

A full-size 3-wall fire whirl prototype, based on the design from Phases I and II, was implemented in a large outdoor environment to investigate the feasibility of using fire whirls for large-scale oil remediation. Both fire whirl and pool fire experiments were conducted to measure the fire dynamics and emissions to refine predictions at large scale. Measurements included temperature measurements of the flame, oil layer and water layer, heat flux measurements near the pool center and on the side, air entrainment velocity, and particle and gas emissions. Videos were taken from four different angles and drone footage was taken from overhead during the experiments. The results from this scale are useful for assessing the scalability, robustness and

efficiency of fire whirls generated at large scales. This stage was designed to serve as a proof-of-concept at technology readiness level (TRL) 5, a technology prototype tested in relevant environments, to suggest opportunities and modifications to future designs for commercial implementation.

Table 4 shows the daily experimental plan outlining the large-scale outdoor experiment. Prior to Day 1, all parties involved in this project worked closely on preparations. On Day 1, experimental configurations were set up, but due to lightning warnings on site in the afternoon, more configuration and instrumentation setup were performed on the morning of Day 2. Preliminary tests using diesel were conducted to check for successful formation of the fire whirl and test the instrumentation in the afternoon on Day 2. After witnessing the success of the diesel fire whirl formation in the configuration, 4 fire whirl tests using HOOPS (2 tests with a 15 mm slick thickness and 2 tests with 40 mm slick thickness) were conducted to ensure repeatable fire whirl formation on Day 3. On Day 4, pool fire experiments were conducted using HOOPS for two slick thicknesses (15 mm and 40 mm) and diesel for comparison.

Table 4 Experimental plan for large-scale outdoor experiment in May 15-19, 2023 at College Station, Texas

<table>
<tr><th></th><th>Day 1 – 05.15</th><th>Day 2 – 05.16</th><th>Day 3 – 05.17</th><th>Day 4 – 05.18</th><th>Day 5 – 05.19</th></tr>
<tr><td>7:00</td><td rowspan="5">Prep – setup site fire whirl config.</td><td rowspan="3">Prep – setup site fire whirl config.</td><td>Setup for burn</td><td>Setup for burn</td><td rowspan="5">Data backup</td></tr>
<tr><td>8:00</td><td rowspan="2">Burn # 2 - HOOPS FW (15 mm)</td><td rowspan="2">Burn #6 - HOOPS PF (15 mm)</td></tr>
<tr><td>9:00</td></tr>
<tr><td>10:00</td><td rowspan="2">Prep – setup instruments</td><td rowspan="2">Burn # 3 - HOOPS FW (40 mm)</td><td rowspan="2">Burn #7 - HOOPS PF (40 mm)</td></tr>
<tr><td>11:00</td></tr>
<tr><td>12:00</td><td colspan="5">LUNCH</td></tr>
<tr><td>13:00</td><td rowspan="5">Lightning strike</td><td rowspan="3">Burn #1 Diesel FW (15 mm)</td><td>Burn #4 - HOOPS FW (40 mm)</td><td>Burn #8 - Diesel PF (15 mm)</td><td rowspan="5">Ship equipment</td></tr>
<tr><td>14:00</td><td rowspan="2">Burn #5 - HOOPS FW (15 mm)</td><td rowspan="2">Clean the site and pack up equipment</td></tr>
<tr><td>15:00</td></tr>
<tr><td>16:00</td><td rowspan="2">Store equipment & adjourn</td><td rowspan="2">Dismantle fire whirl config., store equipment & adjourn</td><td rowspan="2">Demobilization</td></tr>
<tr><td>17:00 until completed</td></tr>
</table>

5.2 Experimental Methodology

The testing site was located at the Brayton Fire Training Field of Texas A&M Engineering Extension Service (TEEX) in College Station, Texas. The latitude and longitude of the site are N 30°34′40” and W 96°21′16”. Fig. 31 shows the site plan and facilities at our experimental field.

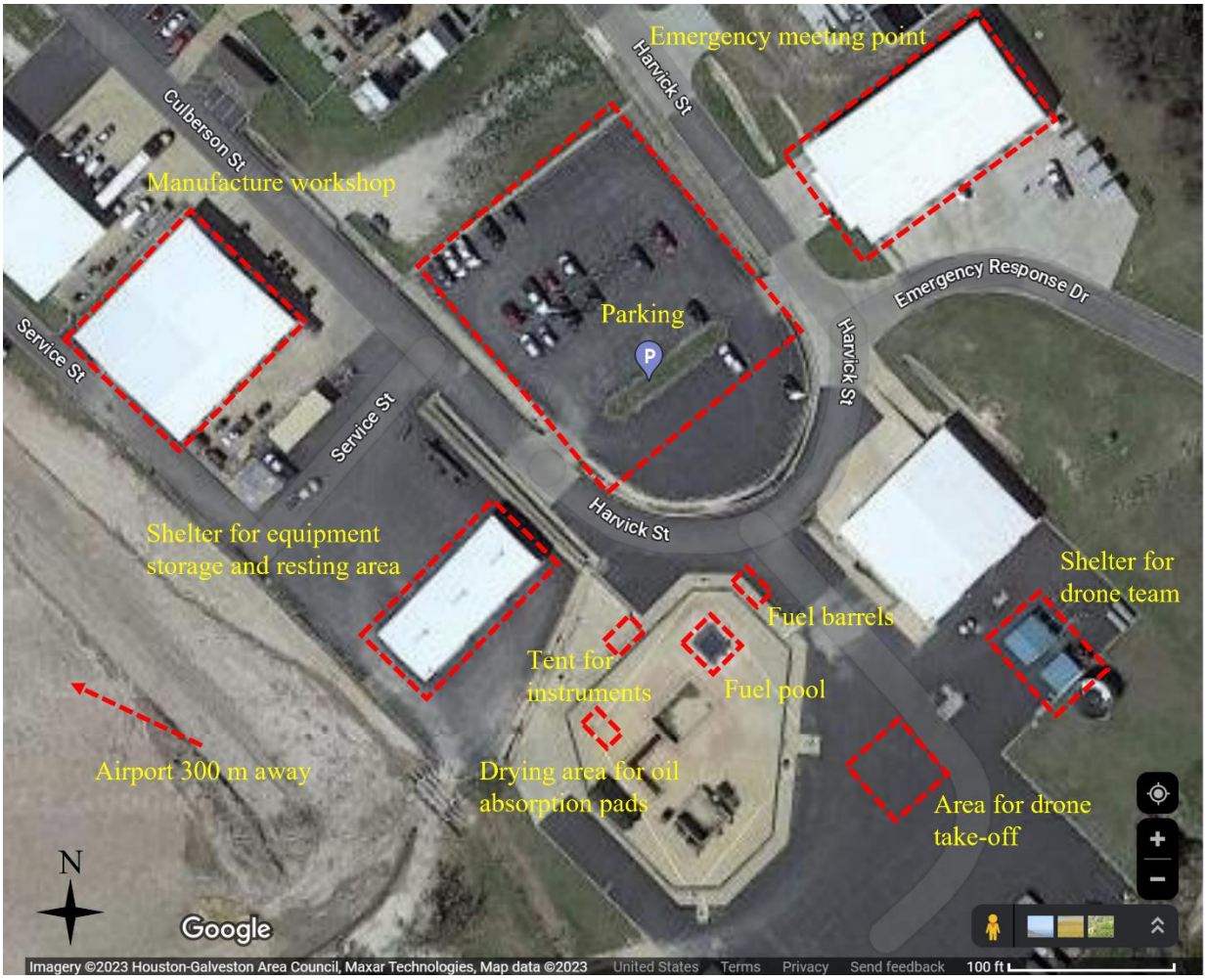

Fig. 31 Site plan
TEEX site plan for the large-scale outdoor experiment

In this large-scale experiment, fire whirls and pool fires were set inside a 1.5 m diameter metal ring filled with fuel, which was suspended at the surface of a 3 m by 3 m wide and 1.2 m deep pool filled with water. A three-wall structure was constructed based on the design of Phase I and II to generate fire whirls. The wall structure was made of fire-retardant wallboard to form a 5 m by 5 m surface with a steel frame for support at the back (Fig. 32 is an aerial photo of the wall structure taken by a drone camera). Three walls formed an equilateral triangle with a single gap of 1.5 m on each side wall to allow for the tangential entrainment of air during burning. The distance from the center of the metal ring to each wall was 1.8 m. Fig. 33 shows the fire whirl configuration plan and locations of instruments in the experiments.

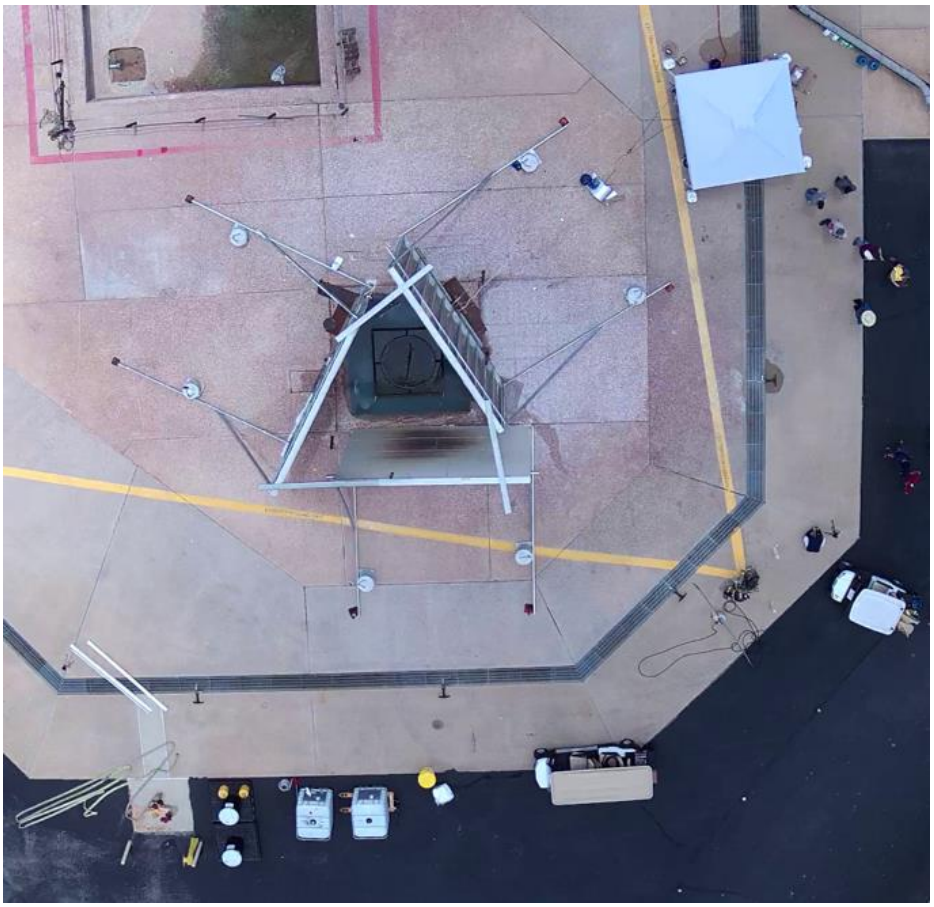

Fig. 32 Aerial photo
Aerial photo of the wall structure and site. (Photo: USGS, 2023)

Six anemometers (Testo 405i) were used at the inlets during fire whirl experiments with three fixed at location A of the wall structure at elevated heights (0.25, 0.5, 1.5 m) to measure the flow velocity inlet into the test section, and one each at location B and C at 0.25 m from the ground. The probe of the anemometer was positioned perpendicular to the wall and 0.4 m from the wall surface. Fig. 33 shows the locations of the anemometers in fire whirl experiments. For pool fire experiments, one anemometer was fixed on an existing pole, 0.25 m from the ground. A portable weather station (Kestrel) was installed 20 m east of the fuel ring to monitor ambient conditions, including wind speed and direction, humidity, and temperature, throughout the whole period of experimental days.

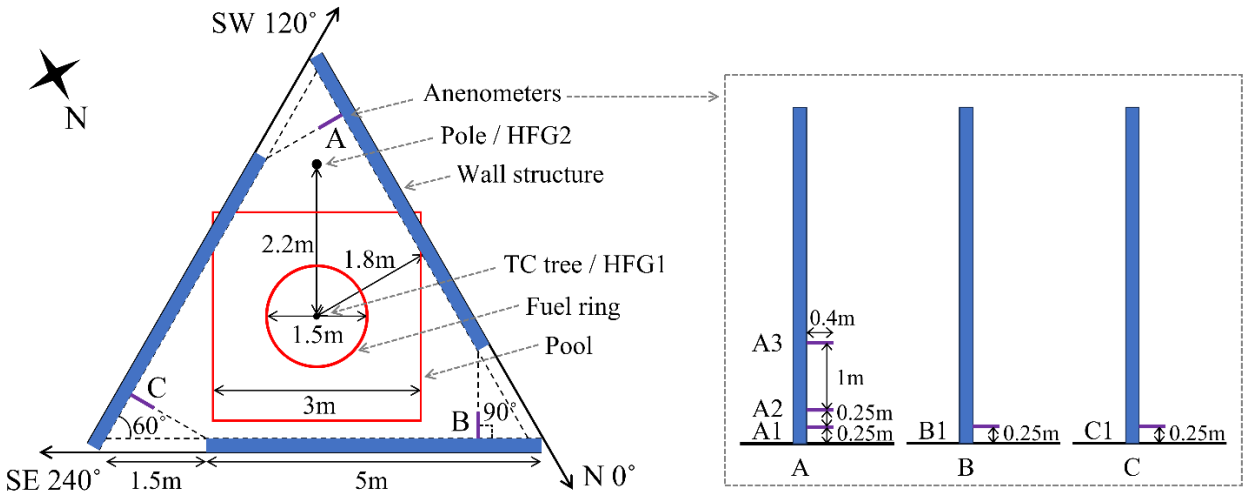

Fig. 33 Configuration and instrumentation
Fire whirl structure configurations and locations of instruments.

A thermocouple tree was built up from the center of the fuel ring to measure the temperature variation within the pool, oil slick thickness, and of the generated flame. In total 14 K-type thermocouples were installed along the TC tree with detailed locations of the thermocouples shown in Fig. 34. Two water cooled total heat flux gauges (Medtherm) were calibrated against a reference gauge using a cone calorimeter at UC Berkeley and used in this outdoor experiment. One heat flux gauge (HFG1) was installed at the thermocouple tree, 15 cm offset and protruding up from the fuel slick surface to capture heat flux feedback from the flame and another on top of the 1.3 m pole which was 2.2 m from the center of the fuel ring, measuring radiation from the flame to the surroundings. Fig. 35 shows the locations of heat flux gauges and TC tree.

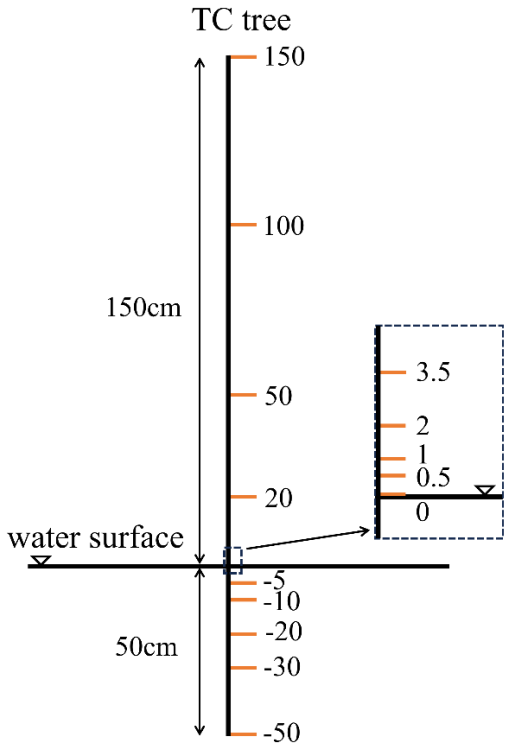

Fig. 34 TC tree
Thermocouple distribution along the TC tree (in cm).

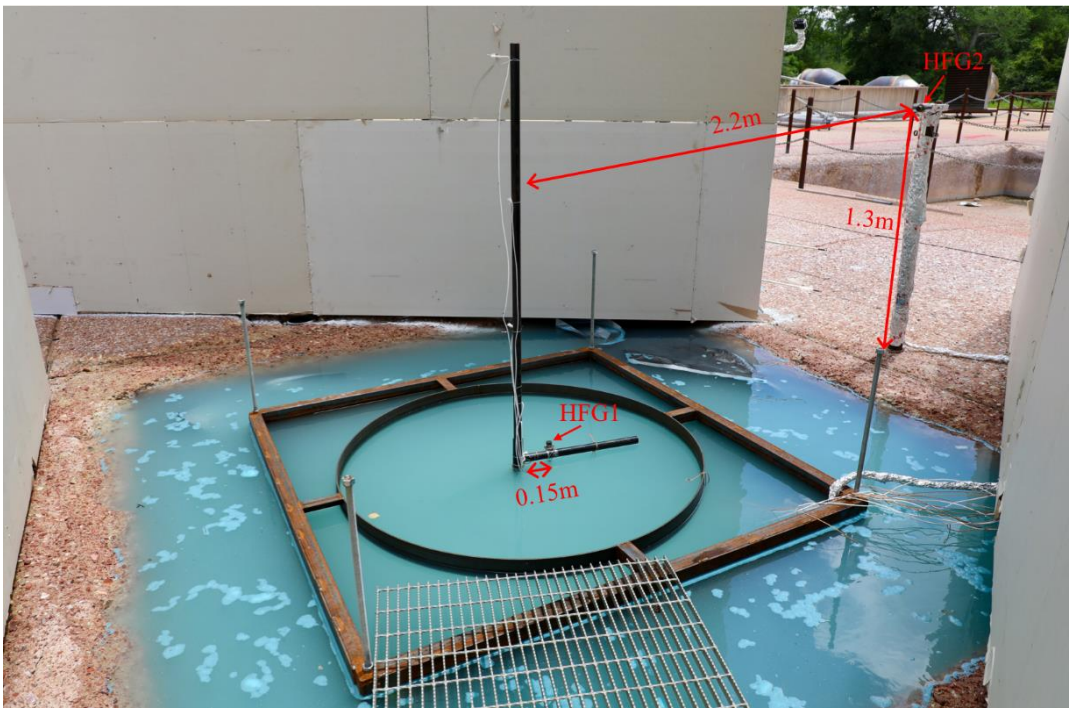

Fig. 35 Locations of HFGs
Photo showing locations of the heat flux gauges and TC tree.

Action and high-speed cameras were set up around the test area to record images and videos of generated fire whirls and pool fires. Fig. 36 shows the layout of six cameras used for these experiments. Camera 1 (GoPro), 2 (Sony high speed camera) and 3 (Casio high speed camera) were set up 7, 12, and 12 m, respectively from the center of the fuel ring to record the videos of the flames. Camera 4 (SJCAM action camera) was mounted at the edge of the wall 1.7 m from the ground facing the fuel ring to record the formation process of fire whirl (Camera 4 was not used in pool fire tests). Camera 5 was mounted on a drone (DJI) and used to record aerial footage. Camera 6 (Canon 5D) was used to take photos to record the flame during experiments.

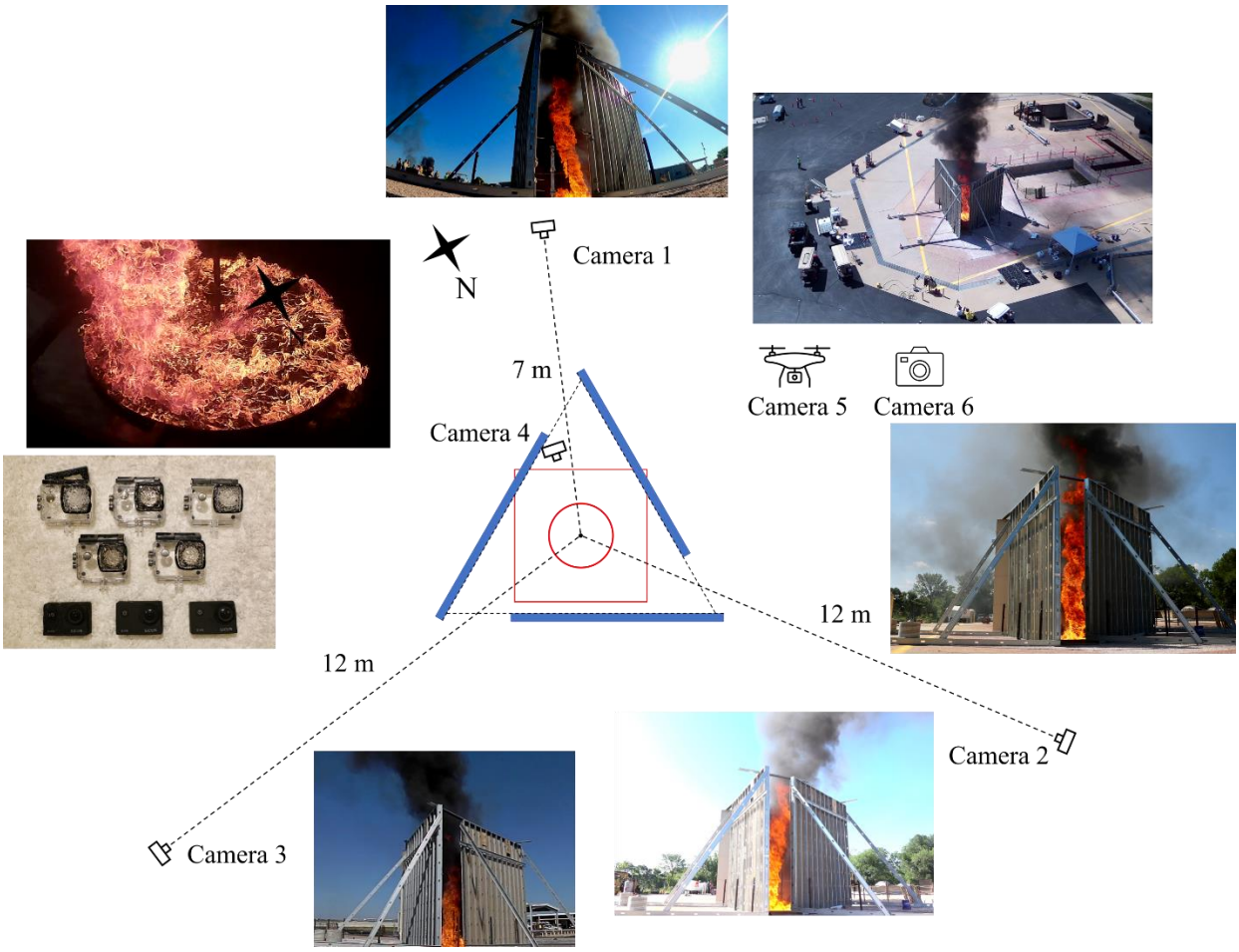

Fig. 36 Camera layout
The layout of six cameras used in large-scale outdoor experiments.

HOOPS, a medium-weight crude oil typical of the Gulf of Mexico was used as the primary fuel for testing. Before the start of experiments using HOOPS, preliminary tests were performed using a surrogate fuel, diesel to confirm the feasibility of the configuration. Experiments using two oil slick thicknesses, 15 mm and 40 mm, were conducted to study the effect of slick thickness on burning efficiency and emissions. The 15 mm thickness represents a limiting case to support combustion while the 40 mm thickness represents a more realistic layer thickness used in

open water burning. The fuel in the fuel ring was ignited using a propane torch in each experiment by TEEX staff. Two fire whirl experiments were performed for each slick thickness and one pool fire experiment was performed for each slick thickness using HOOPS. The mass of crude oil used for each experiment was measured by a mass balance on site. The residues of crude oil were collected by using 3M sorbent pats and weighed after air drying overnight to determine the mass of remaining crude oil after burning. Samples of the raw crude oil and residues after burning in each condition were taken back to UC Berkeley for elemental analysis (CHN) after experiments were completed.

Emissions monitoring was handled by external partners, led by the Environmental Protection Agency (EPA) with the US Geological Survey (USGS) supporting drone piloting. Emission data was collected by using air quality sensors and particle sampling onboard drones flown over experiments. CO_2 and CO were measured inside the plume for each experiment while PM was collected on filter samples for later analysis. Table 5 presents a list of targeted emissions along with their respective sampling methodologies. The data analysis for emissions is handled by the EPA and the results from a report provided by EPA are summarized in Section 5.4 [Karen: note we want to update with a reference once EPA tells us this is finalized but they have not yet].

Table 5 Targeted Emissions and Sampling Methods

Analyte	Instrument/Method	Frequency
CO_2	K30 FR, NDIR	Continuous
CO	E2V EC4-500-CO, Electrochemical cell	Continuous
$PM_{2.5}$	PEM Impactor, Teflon filter, gravimetric	Batch
EC/OC/TC	PMI impactor, Quartz filter, thermal-optical	Batch

In total, 8 experiments were performed and are named Burn 1 to Burn 8. Table 6 summarizes the experimental matrix from Burn 1 to Burn 8 and lists the time, mass of the fuel and measurements performed for each test condition.

Table 6 Experimental matrix for the large-scale outdoor experiment

	Date	Time	Fuel	Type of Burn	Targeted Slick Thickness (mm)	Weight of Fuel (kg)	Measurements
Burn 1	05/16	14:00	Diesel	FW	15	31.8	1-3, 5-7
Burn 2	05/17	09:00	HOOPS	FW	15	36.1	1-7
Burn 3		10:48	HOOPS	FW	40	65.5	1-7
Burn 4		13:59	HOOPS	FW	40	63.6	1-7
Burn 5		15:30	HOOPS	FW	15	36.2	1-7
Burn 6	05/18	08:34	HOOPS	PF	15	37.3	1-7
Burn 7		10:13	HOOPS	PF	40	65.6	1-7
Burn 8		13:05	Diesel	PF	15	31.8	1-3, 5-7

Measurements:

1. Temperature. 14 TCs.
2. Heat flux. 2 HFGs.
3. Flow velocity. 5 anemometers in FW and 1 anemometer in PF.
4. Mass consumption.

5. Videos and photos.
6. Emissions. EPA and USGS.
7. Ambient conditions. Weather station.

5.3 Experimental Results

All fire whirls in our experimental plan were successfully formed in the large-scale experiments (Burn 1 - 5), including one fire whirl with diesel and four fire whirls with HOOPS (two each at 15 mm and 40 mm slick thickness). Fig. 37 shows a photo of a successful fire whirl and pool fire formed in the large-scale experiment, side-by-side. Fig. 38 shows a fully formed fire whirl or pool fire for each experiment. This section presents the results of the experimental measurements on the ground with emissions measurements from the EPA.

Fig. 37 Fire whirl vs pool fire
Photos of a successfully-formed fire whirl and pool fire during the large-scale experiments.

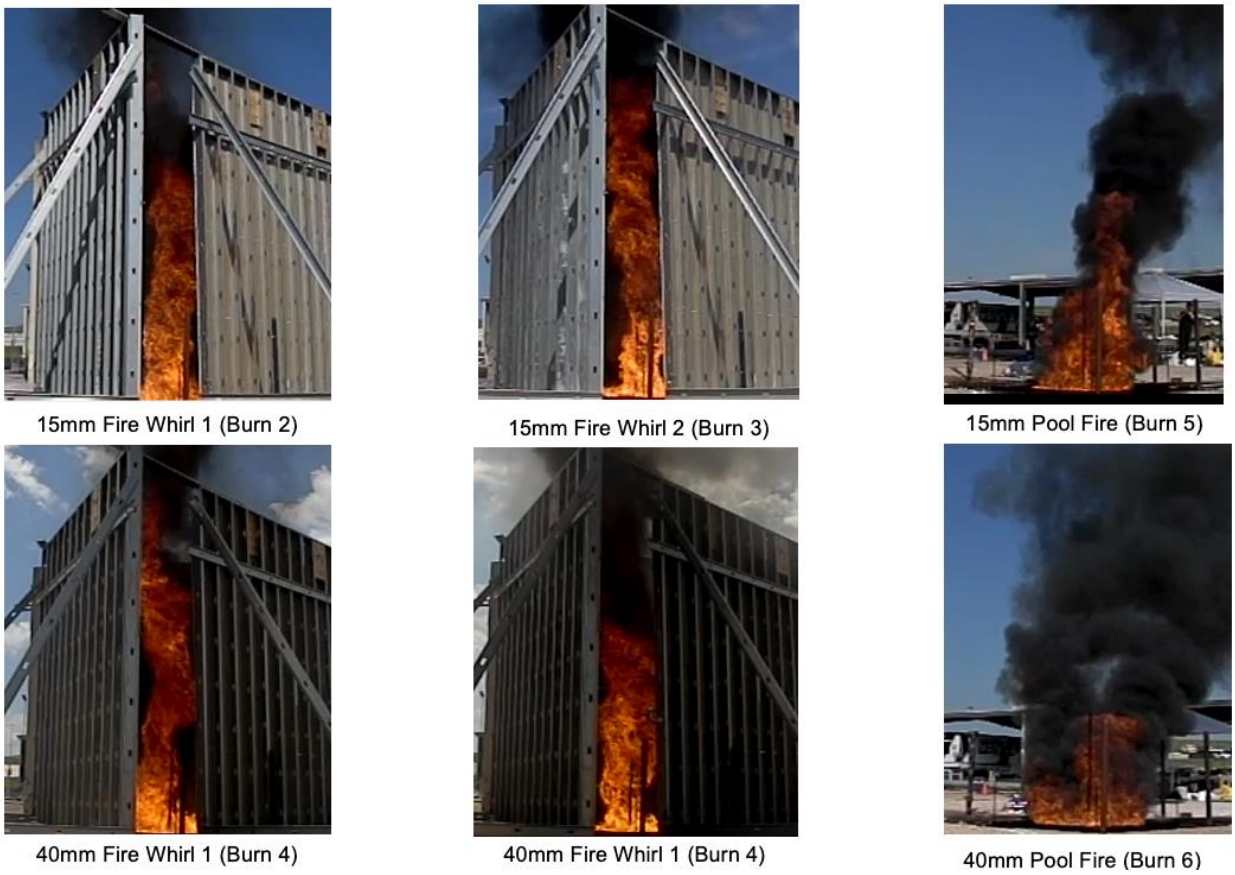

Fig. 38 Photos of large-scale crude oil burn
Photos taken from video of all 6 crude oil fire whirl and pool fire experiments are shown for both 15 mm and 40 mm fuel slick thicknesses.

As described in objectives, this large-scale outdoor experiment is designed to help inform future implementation of more efficient ISB practices. Not only is the scale of this fire whirl experiment important, the influence of outdoor ambient conditions on the fire whirl dynamics provides an important reference for future studies, differing from previous laboratory studies where ambient conditions were carefully controlled. From the recording of weather during these experiments, the ambient conditions were relatively stable, with temperatures varying in the range from 24 to 32 ℃ and humidity from 43 to 71%. No burns were conducted during precipitation. Wind conditions were recorded by a weather station 20 m from the center of the fuel ring. The wind speed and direction for all crude oil experiments are shown in Fig. 39. The ambient wind condition for a pool fire of 15 mm slick thickness was below 1 m/s blowing from the north, while for the 40 mm slick thickness the wind speed was up to 2 m/s and the direction varied from the southwest to the north. For the fire whirl experiments, the wind speed for two experiments using a 15 mm slick thickness ranged from 0.8 to 1 m/s, while for two experiments with a 40 mm slick thickness the wind speed was up to 3 m/s.

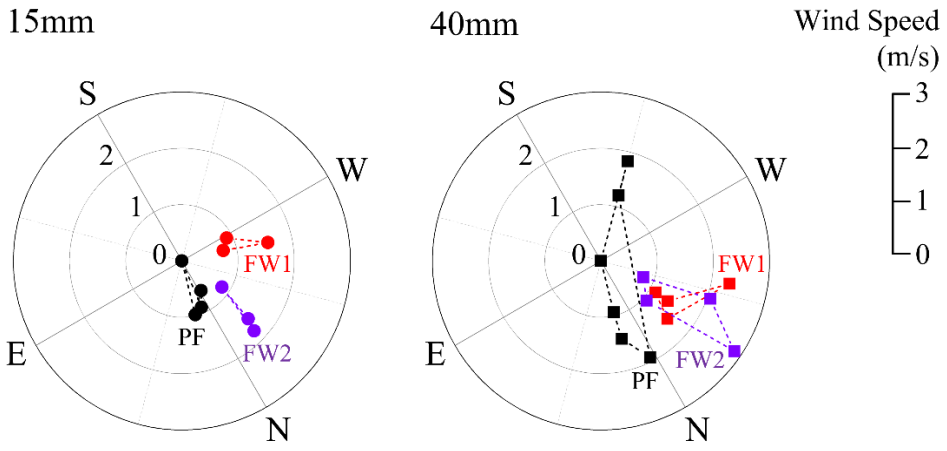

Fig. 39 Ambient wind conditions
Ambient wind speed and direction during the fire whirl and pool fire experiments of HOOPS. Each point represents a wind speed measurement once every 5 minutes for a specific test (labeled with individual colors). The further out from the center of the circle indicates how high the wind speed was, while the direction of the points on the circle indicates the direction the wind speed came from.

Anemometers were used to record the flow velocity and temperature moving into the test section for each experiment, providing a relative measure of air entrainment for each burning condition and, for fire whirls, an assessment of circulation or swirl. Fig. 40 shows the flow velocity and temperature measured at three elevated heights, 0.25, 0.5, and 1.5 m from the ground at opening A of fire whirl experiments for four crude oil fire whirl experiments. The results show that the flow velocity varies at different heights along the air inlet, in general, higher at 0.25 m from the ground, which agrees with our findings in laboratory experiments. The results from anemometers at three openings 0.25 m from the ground show variations too (shown in Fig. 41). The maximum flow velocity recorded in fire whirl experiments was 25 m/s, while the flow velocity in pool fire experiments did not show an obvious increase in velocity (shown in Fig. 42). It is important to note the limitations of the anemometers used. They were selected based upon their ability to remotely record and transmit velocity data with temperature corrections and were used in previous experiments. However, they were limited to a working temperature of up to 60℃ and a velocity of up to 30 m/s. The maximum velocity measured may therefore be limited by both the temperature cutoff and the total range of the device. Our results, however, show obvious differences in air entrainment when comparing fire whirls and pool fires.

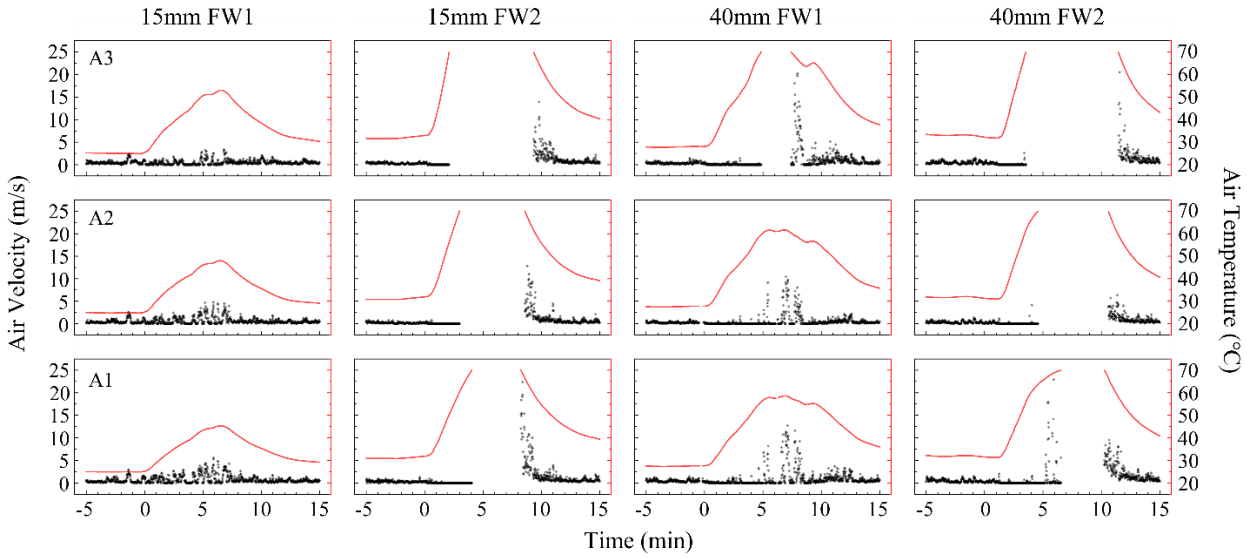

Fig. 40 Flow velocity and temperature at different height
Flow velocity and temperature measured by anemometers at elevated heights, 0.25, 0.5, and 1.5 m from the ground at opening A during fire whirl experiments. Data points were interrupted when the temperature was higher than the working temperature threshold of the anemometer.

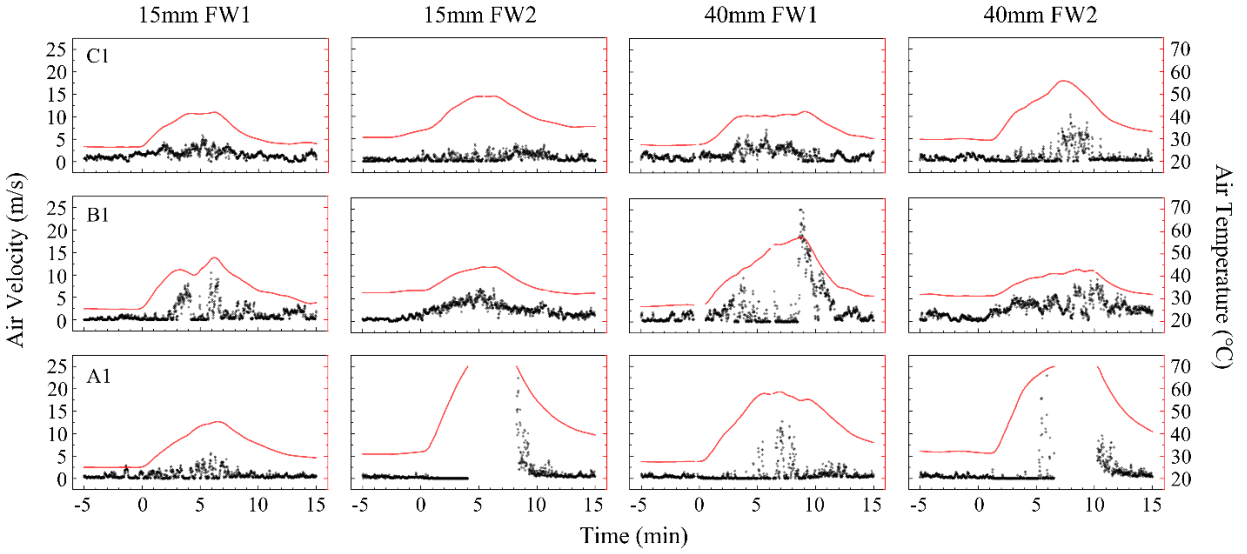

Fig. 41 Flow velocity and temperature at different opening
Flow velocity and temperature measured by anemometers at openings A, B and C, 0.25 m from the ground during fire whirl experiments. Data points were interrupted when the temperature was higher than the working temperature threshold of the anemometer.

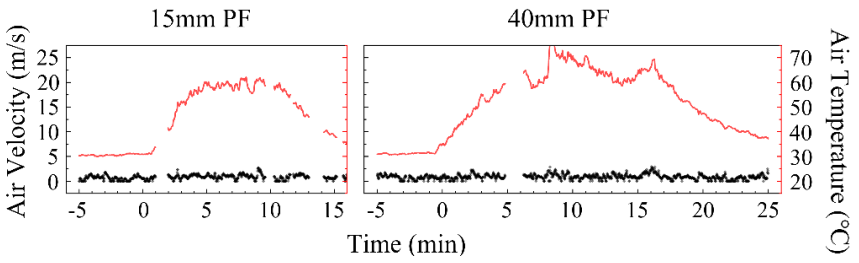

Fig. 42 Flow velocity and temperature for pool fire
Flow velocity and temperature measured by an anemometer fixed at the pole, 0.25 m from the ground during pool fire experiments. Data points were interrupted when the temperature was higher than the working temperature threshold of the anemometer.

Fig. 43 shows examples of the temperature profiles measured during one fire whirl and one pool fire experiment with a 40 mm slick thickness of HOOPS. These selected heights for temperature measurements represent the typical variations of temperature in the flame, in the oil, and in the water. The thermocouple TC150 shown was located 150 cm above water surface, representing the temperature of the flame at 1.5 m from the fuel. Because the weight of the crude oil made the water surface descend during the experiments, TC3.5 was exposed initially at the surface of the fuel, representing the temperature of the flame at the fuel surface. From the results in Fig. 43, the maximum temperature of the flame recorded in the fire whirl was 1000°C, and the maximum temperature in the pool fire was 850°C. The maximum temperatures were all recorded at the fuel surface. Because the height of the flame in fire whirls is higher than that in pool fires and the flame inclination of the pool fire was more easily influenced by the ambient wind, temperature difference between the fuel surface and 1.5 m above fuel surface is higher in fire whirl experiments. TC1 and TC0.5 represent the temperature variation in the slick thickness of burning oil. The results show that the temperature increase of the fuel during the fire whirl is faster than the pool fire, indicating increased heat feedback from the flame to the fuel surface. TC0 represents the temperature at the fuel water interface and TC-5 represents the temperature less than 5 cm below the water surface. The results show that the distance of thermal penetration into the water is higher in fire whirl experiments, and that the water reaches a boiling temperature only in fire whirl experiments.

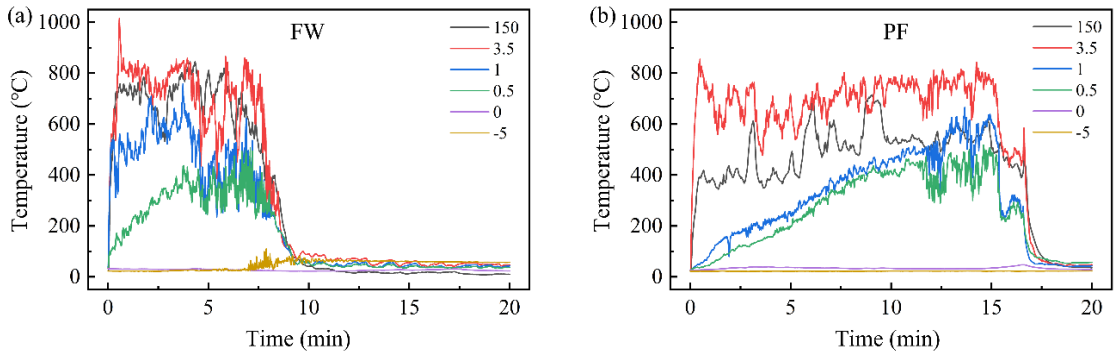

Fig. 43 Temperature profiles
Temperature profiles at selected heights for fire whirl (a) and pool fire (b) experiments. TC150, 3.5, 1, 0.5, 0, -5 are thermocouples at the height 150 cm, 3.5 cm, 1 cm, 0.5 cm, 0 cm, -5 cm from the water surface in experimental design.

Fig. 44 shows the total heat flux measured near the center of the flame above the fuel surface (HFG1) and 2.2 m away from the center facing the flame (HFG2) for all experiments. In this large-scale experiment, the measured total heat flux from the flame to the sensor near the fuel surface in fire whirl experiments was found to reach more than 300 kW/m^2, which is significantly higher than the heat flux measured in pool fires. Due to both an elongated flame and possible re-radiation within the enclosure higher values should occur. These heat fluxes, however, are significantly higher than traditionally expected and beyond the calibration range of the devices (150 kW/m^2). Sandia National Laboratory, however, has done heat flux measurements from fire whirls formed in a wind tunnel using a 1.77 m square fuel pan and measured up to 396 kW/m^2 at the ceiling above the flame (Luketa 2018). While the trends and differences between pool fires and fire whirls are clear, these results are still more than double the calibration range of the sensor and should be interpreted with caution until further field-scale verification can be performed.

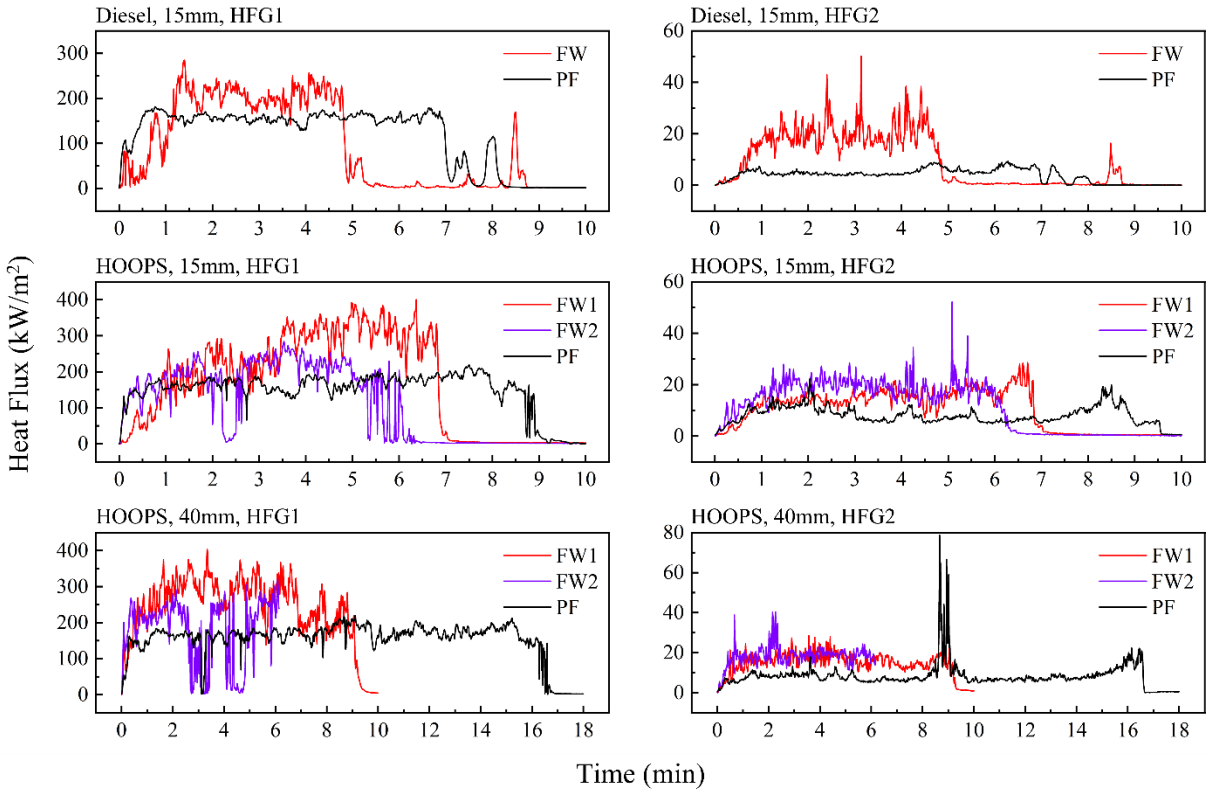

Fig. 44 Heat flux measurements
Heat flux at the center of the fuel ring and 2.2 m away from the center in fire whirl and pool fire experiments.

Fig. 45 shows comparisons of the fuel consumption efficiency for all cases in the experiments using HOOPS, calculated by dividing the initial mass of the fuel by the mass burned. The results show that, for a slick thickness of 15 mm, fire whirl experiments show slightly higher fuel consumption efficiency than pool fire experiments, while for the 40 mm slick thickness, fire whirl experiments show lower fuel consumption efficiency. Comparing the fuel consumption efficiency between slick thickness, fire whirl experiments of 15 mm slick thickness show higher

values, while the pool fire experiment of 40 mm slick thickness show higher values than the 15 mm slick thickness. Laboratory experiments, however, found increasing slick thickness results in an increase of fuel consumption efficiency and the fire whirl configuration has a higher fuel consumption efficiency than the pool fire configuration. The results we obtained from large scale experiments are different, therefore, than the results from laboratory studies. There are several potential reasons for this variation. First and foremost, the wind conditions were significantly different for the 40 mm pool fire. Fig. 39 shows that in experiments with a 40 mm slick thickness, the wind speed and direction was both much greater than in experiments of the 15 mm slick thickness and experienced greater variations in wind speed. Visual observations support this as the plume experienced significant “tilting” downwind. A higher wind speed can push the fire and plume close towards the fuel surface, increasing heat feedback and therefore increasing the fuel consumption efficiency of pool fire burning. For fire whirls, this may make air entrainment of the fire whirl more asymmetric and complicated, affecting burning efficiency in unknown ways. A second reason could be because of the dimension of the fuel ring. The fuel ring was designed to be 1.2 m diameter based on optimized burning conditions from our laboratory experiments. The as-built diameter by on-site manufacturing was instead 1.5 m based on available materials and they were unable to change the size of the ring. As the size of the walls were also fixed, we could not move the walls further to keep the distance designed between the edge of the fuel ring and the wall. This made the distance between the fire whirl and the wall too close, restricting some air entrainment to the fire whirls. This may have also caused a compounding effect with instability generated by imposed winds. While conditions were not optimal, it is expected in field conditions non-optimal conditions would naturally arise, so these results still provide a realistic test case and demonstration of the technique, even if not fully optimized.

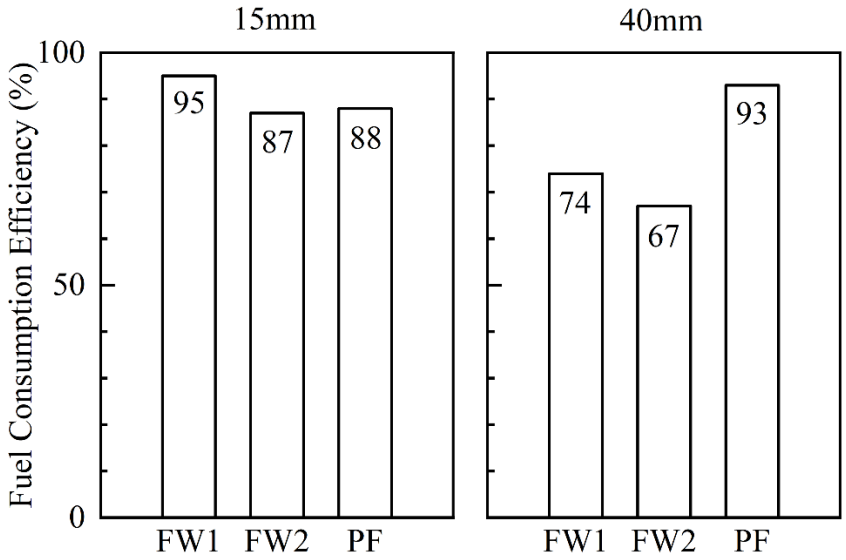

Fig. 45 Fuel consumption efficiency
Fuel consumption efficiency of fire whirl and pool fire large-scale experiments.

Table 7 presents the results of elemental analysis for residue sample collected after burning and the original crude oil used in the field experiments. The results from samples of HOOPS and ANS used in the lab in experiments of Phase I and II are added for comparison. The mass fraction of oxygen is calculated by subtracting other components by 100 percent. Generally, HOOPS is shown to have about 85-86% carbon content before burning and 77-82% carbon content in the remaining residue. This suggests that there has been relatively limited volatilization of the remaining crude suggesting a large effect on extinguishment of the flame before remaining excesses are burned off. The results also show, comparing to the original crude oil used in the field, residue samples have a higher oxygen fraction. The residue is more oxidized in the test condition of the pool fire compared to the fire whirl with the same slick thickness.

Table 7 Results of elemental analysis for residue and original crude oil

		C (%)	H (%)	N (%)	O (%)
Residue	15mm FW	82.4 ± 0.2	11.3 ± 0.0	1.6 ± 0.1	4.7
	15mm PF	77.3 ± 0.1	11.2 ± 0.0	1.0 ± 0.1	10.5
	40mm FW	80.3 ± 0.2	11.4 ± 0.0	1.4 ± 0.1	6.8
	40mm PF	81.2 ± 0.4	10.8 ± 0.0	0.5 ± 0.2	7.4
Original	HOOPS (field)	85.9 ± 0.2	12.6 ± 0.1	1.1 ± 0.1	0.4
	HOOPS (lab)	85.8 ± 0.1	8.2 ± 0.2	0.9 ± 0.1	5.1
	ANS (lab)	86.0 ± 0.1	12.3 ± 0.1	0.7 ± 0.1	1.0

5.4 Emissions Measurements

The EPA conducted emissions measurements and analyzed the emission data. Table 8 summarizes the results of gas and particle emissions in all tests conducted in this field experiment. Measurements included measurement of CO and CO_2 as well as collection of $PM_{2.5}$ on a drone-based platform during the experiments. Results were expressed as emission factors (EF) representing the mass of the analyte divided by the mass of oil burned as well as a modified combustion efficiency (MCE) using a more traditional formulation with just CO and CO_2,

$$MCE_G = \frac{\Delta CO_2}{\Delta CO_2 + \Delta CO} \quad \text{Eq. 1}$$

or by also including the total carbon adding the $PM_{2.5}$ to the denominator,

$$\boldsymbol{MCE_T = \frac{\Delta CO_2}{\Delta CO_2 + \Delta CO + TotalCarbon}} \quad \text{Eq. 2}$$

The MCE_G values from the test burns are quite similar (~ 1% range variation), while the MCE_T values are less similar (a 4% range variation), ranging from 0.874 to 0.913, indicating that the PM carbon content is responsible for greater variation in the tests' combustion efficiencies. In

general, emissions of fire whirls have a higher combustion efficiency than pool fires. Fig. 46 shows the $PM_{2.5}$ emission factors from pool fires are 40% higher than the emission factors from the fire whirls.

The TC/EC/OC (Total Carbon/Element Carbon/Oxygen Content) emission factors determined from analysis of filter samples are shown in Table 9. On average, 75% of the $PM_{2.5}$ mass was carbon from the crude oil - fire whirls, of which 86% was elemental carbon.

Table 8 Emission factors of CO_2, CO and $PM_{2.5}$ and MCE from each of the tests

	Test Condition	CO_2		CO		$PM_{2.5}$		MCE	
		g/kg oil initial	g/kg oil consumed	g/kg oil initial	g/kg oil consumed	g/kg oil initial	g/kg oil consumed	MCE_T	MCE_G
1	Diesel – Fire Whirl: 15mm	2661	2661	43	43	96.2	96.2	0.875	0.975
2	HOOPS – Fire Whirl: 15mm	2672	2812	44	47	76.6	80.6	0.893	0.976
3	HOOPS – Fire Whirl: 40mm	2890	3935	44	61	53.1	72.3	0.897	0.977
4	HOOPS – Fire Whirl: 40mm	2902	4363	43	64	76.6	115.2	0.913	0.978
5	HOOPS – Fire Whirl: 15mm	2757	3178	45	51	72.1	83.1	0.895	0.977
6	HOOPS – Pool Fire: 15mm	2723	3096	45	51	111.9	127.3	0.874	0.976
7	HOOPS – Pool Fire: 40mm	2566	2764	59	64	120.7	130.0	0.891	0.973
8	Diesel – Pool Fire: 15mm	2687	2687	44	44	92.7	92.7	0.857	0.977

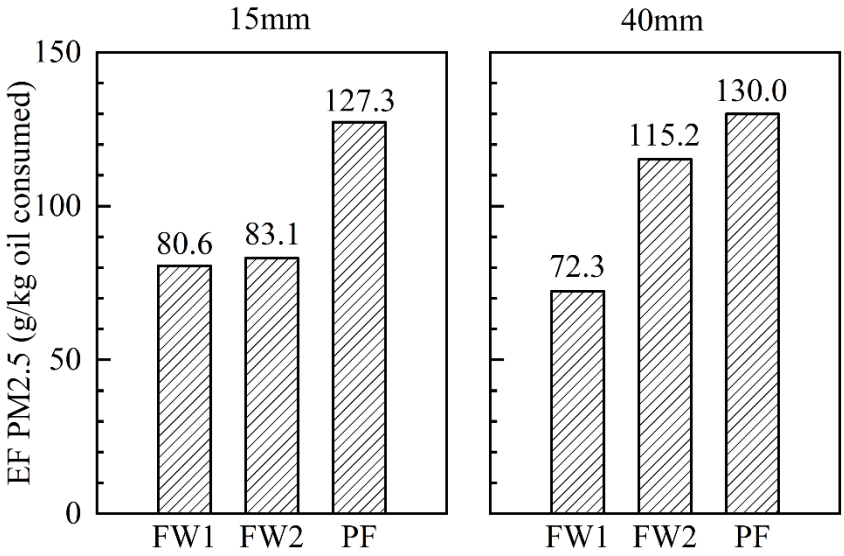

Fig. 46 EF $PM_{2.5}$
Emission factors of $PM_{2.5}$ for fire whirls and pool fires in large-scale experiments.

Table 9 Total carbon, elemental carbon, and organic carbon emission factors.

Burn No.	Test Condition	OC	EC	TC	OC	EC	TC
		g/kg oil initial			g/kg oil consumed		
1	Diesel – Fire Whirl: 15mm	12.3	82.3	94.7	12.3	82.3	94.7
2	HOOPS – Fire Whirl: 15mm	NS	NS	NS	NS	NS	NS
3	HOOPS – Fire Whirl: 40mm	11.2	63.3	74.5	15.3	86.2	101.5
4	HOOPS – Fire Whirl: 40mm	9.8	48.2	58.0	14.8	72.5	87.2
5	HOOPS – Fire Whirl: 15mm	9.0	67.6	76.6	10.4	77.9	88.3
6	HOOPS – Pool Fire: 15mm	14.7	78.3	92.9	16.7	89.1	105.7
7	HOOPS – Pool Fire: 40mm	7.8	65.0	72.8	8.4	70.0	78.4
8	Diesel – Pool Fire: 15mm	18.7	97.6	116.3	18.7	97.6	116.3

Note: NS = not sampled.

5.5 Discussions on the Large-Scale Experiments

Overall, the large-scale fire whirl experiments in Texas were a success in terms of project objectives. We generated repeatable fire whirls and pool fires, were able to capture all desired experimental results, and everything was conducted safely and within the specified time and budget. Fire whirls clearly generated significantly higher heat fluxes to the fuel surface, higher temperatures, and more opaque plumes (shown in Fig. 47). $PM_{2.5}$ emission factors were also around 40% lower for fire whirls compared to pool fires. What was unexpected is a decreased fuel burning efficiency for the fire whirls under 40 mm fuel thickness rather than 15 mm thickness. This indicates serious potential issues with the technique or the specific experiment that will be discussed in this section.

Fig. 47 Photos of the smoke
Photos showing the color of the smoke plume from a fire whirl and pool fire during the large-scale experiments. The smoke of fire whirl is more opaque.

As described in previous sections, large-scale results achieved several objectives of the project, including the successful and repeatable formation of fire whirls at larger scales, reduced particulate emissions, and higher heating rates. While many of these measures indicated higher burning efficiencies, the goal of in-situ burning is to remove the maximum amount of oil spilled over a liquid surface. This was not achieved in 3 of 4 fire whirl tests as shown in Fig. 45 with the second fire whirl test with a 15 mm slick thickness and both fire whirl tests with the 40 mm slick thicknesses not achieving high consumption efficiencies. This therefore leads to some doubts on the methodology being applied to the large scale. However, the highest fuel consumption efficiency was achieved for a 15 mm fire whirl (95%), which suggests that fire whirls have the potential to achieve both high consumption efficiencies and high burning efficiencies, however something occurred in 3 of the 4 fire whirl tests that disrupted this process. We therefore want to explore what may have happened during these tests and present preliminary analysis of these processes.

There are multiple factors that may influence burning efficiency. The configuration sizing, external wind, or changes in pool boilover behavior all may influence the process, or perhaps a combinations of these influences. Due to the fact that one fire whirl presented the highest fuel

consumption, it is hypothesized that fire whirls still have the potential for peak efficiency but that factors influencing the burning process disrupted these conditions at some point during subsequent fire whirl tests. In particular, observation of video footage suggests that this may have been due to early extinguishment of the fire whirl due to external factors. To further investigate this, we have tried to explore each potential external influence to evaluate what potential mechanisms may be at play. Below we have outlined the key factors we have explored that may play a role.

There are several mechanisms that may be responsible for poor fuel consumption efficiency in the tests:

1. The fuel dish size was incorrectly sized, too large for the established walls and footprint.
2. Air entrainment may have been comparatively limited, with too much fuel produced for the amount of air that can enter into the chamber. This is tied to (1).
3. The vortex may have lacked space to develop, hitting the wall (Fig. 48shows the color pattern of the walls after fire whirl experiments), losing heat, distorting the shape, and reducing general efficiency. This is tied to (1).
4. Wind variability could blow the forming whirl to one side or prevent it from forming, or interrupt the vortex it when it was formed and push it to the wall.
5. Pool boilover with thicker fuel layers may have reached some other limit that caused boilover, causing water to agitate and extinguish the flame.
6. Assuming the flame is close to a Burger's vortex, change in circulation could cause interference with the vortex formation since circulation scales with radius, which has changed.

Fig. 48 Photos of the walls after experiments
Photos show the color patterns of the three walls after fire whirl experiments. Fire whirls constantly hit the walls during the experiments.

First, we have explored whether fire whirls burned more efficiently than pool fires and compared these results to small-scale observations that motivated these experiments. To determine burning rates, we estimated an average surface mass flux by evaluating the initial and final mass divided by the duration of burning determined by video measurements. These are very rough estimates, however overhead CO_2 measurements were not total (they were collected only in a location within the plume); therefore, this was the only method available.

Figure 50 shows the average mass loss rate of both the large and small-scale experiments in terms of a mass flux from the fuel surface, with triangles indicating fire whirls and open circles indicating pool fires. The average mass loss rate per unit surface area (mass flux) of the large-scale experiments was calculated as

$$\dot{m}" = \frac{m_{consumed}}{T_{burn} * A_f} \quad \text{Eq. 3}$$

where $m_{consumed}$ represents the difference between the initial mass of oil and residue mass, T_{burn} represents the burn duration in seconds and A_f represents the fuel surface area. Also included in Figure 6.2 is a correlation for the surface mass flux from (Garo et al. 1999) for a 10 cm diameter pool calculated via Eq. 4, and the estimated surface mass flux of a 10 cm pool of oil from (Hurley et al. 2015), shown in Eq. 5.

$$\dot{m}" = \frac{1}{H_v}\left[\chi\left(\frac{4\rho_\infty C_p \left(T_\infty g \left(T_F - T_\infty\right)\right)^{0.5}}{\pi} d^{0.5} - \frac{\alpha_F \lambda_F \left(T_S - T_\infty\right)}{y_{s,i}\left(\alpha_F^{0.5} + \alpha_W^{0.5}\right)^2}\right)\right] \quad \text{Eq. 4}$$

$$\dot{m}" = \dot{m}_\infty" e^{-k_\beta D} \quad \text{Eq. 5}$$

In Eq. 4 to get the surface mass flux, H_v is the heat of vaporization of crude oil, χ is the heat feedback fraction, ρ_∞ is the density of ambient air, C_p is the specific heat of ambient air, T_∞ is the temperature of ambient air, g is the acceleration due to gravity, T_F is the fuel surface temperature, d is the pool diameter, α_F is the thermal diffusivity of the fuel, λ_F is the thermal conductivity of the fuel, T_S is the vaporization temperature of the fuel, $y_{s,i}$ is the initial fuel slick thickness, and α_W is the thermal diffusivity of the water in the water layer. In Eq. 5, is the empirically determined surface mass flux of a theoretically infinite pool, k_β is an empirically determined constant, and D is the pool diameter.

Investigating Fig. 49 we see that fire whirls achieved significantly higher burning rates than pool fires in the laboratory, increasing with slick thickness, while moderate improvements were noted for fire whirls over pool fires at large scale, however the improvement seen for fire whirls with increasing slick thickness does not appear at large scale. At this time, it is unclear why the improvement in burning efficiency with slick thickness that was observed for fire whirls at the laboratory scale does not appear for fire whirls at the largest scale. Furthermore, the burning rates per unit area shown match small-scale experiments, while we would expect significantly increased burning rates based on correlations from (Garo et al. 1999), we actually see reasonable agreement from large pool fire correlations without a water sublayer, suggesting these results at small scale may have other influences. The overall conclusion, however, is that fire whirls do achieve higher burning rates and that less vigorous burning does not seem to be the cause of the remaining unburned fuel.

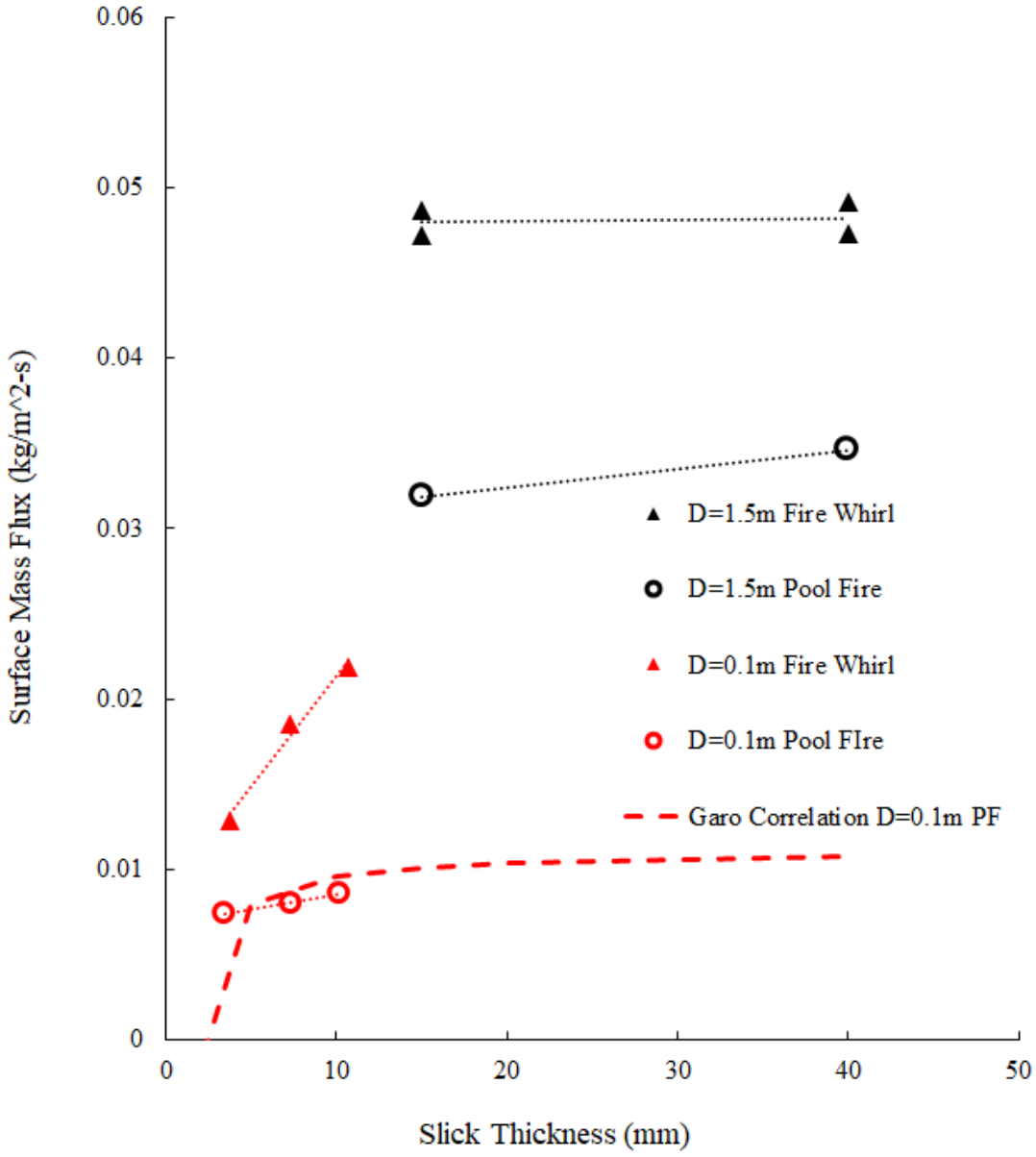

Fig. 49 Surface mass flux comparison
Surface mass flux comparison for the small-scale tests (red) and large-scale tests (black), Including comparisons to analysis from literature.

We have also looked at the emission factors of $PM_{2.5}$ in large and small-scale experiments with different slick thickness, shown in Fig. 50. Similar to small-scale experiments the EFs of fire whirls were significantly lower than pool fires, however, the dependence on slick thickness was not very apparent while it was at small scale.

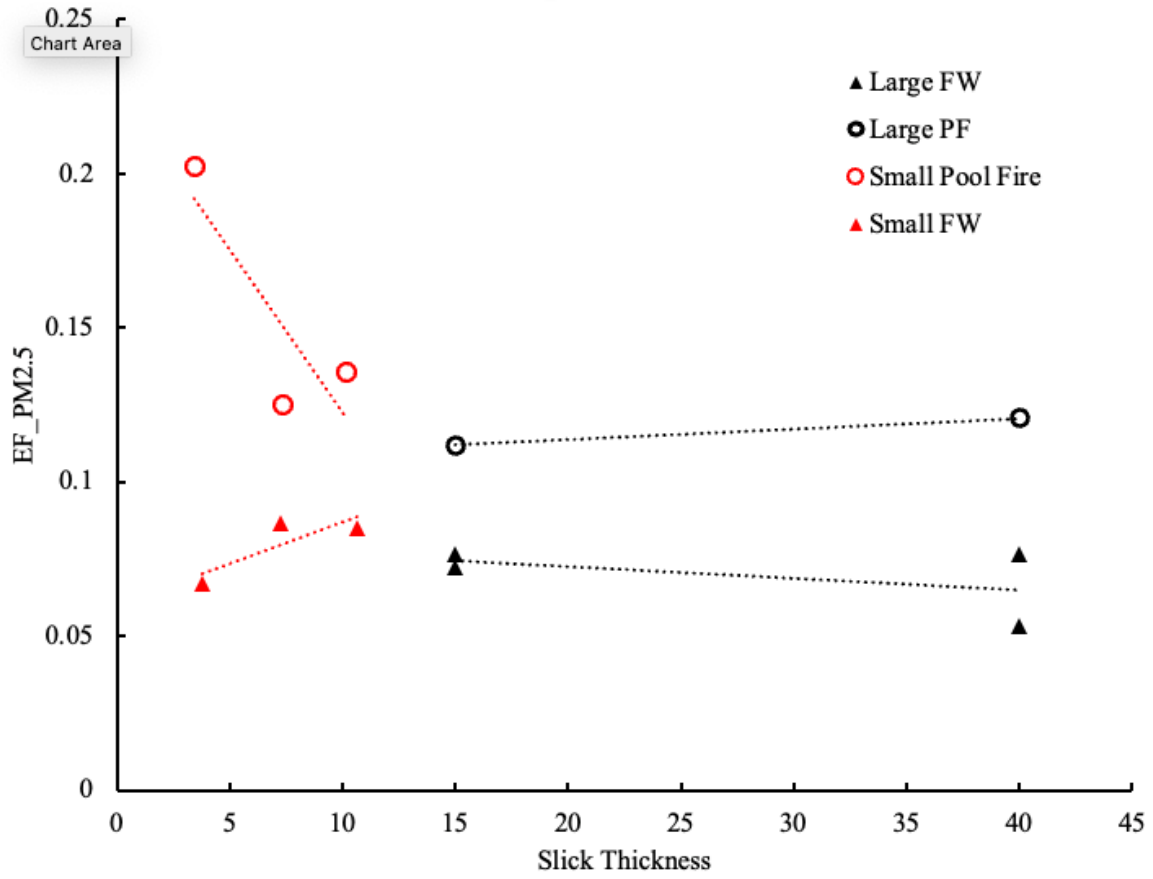

Fig. 50 EF $PM_{2.5}$ across scales
EF $PM_{2.5}$ in large and small-scale experiments with different slick thickness.

Looking back at Fig. 38, it is shown that fire whirls were successfully formed for all fire whirl configurations, so formation alone was not an issue for the modified dimensions used during testing. At extinguishment all fire whirls appeared to decay in rotation and flame intensity. It was difficult to distinguish differences between tests that had higher vs. lower flame consumption, however 40 mm experiments produced thicker smoke plumes and may have been more easily under-ventilated at extinguishment.

Laboratory experiments have been conducted on fire whirls with wind and different wall sizing to determine how these configurations affect fire whirl activity and extinguishment. Fig. 51 and Fig. 52 show unsteady phenomenon in tests using a correctly and further-spaced fire whirl generator under additional wind conditions. Fig. 53 shows the heat release rate (HRR) calculated from the results of gas emissions for these tests. These tests were conducted using heptane to ensure repeatability, so they do not extinguish with a residue. Wind showed significant effects on stability of the fire whirl, regardless of the sizing of the fire whirl generator. Winds were higher on later tests so there is a potential that this played some influence, especially as the oil slick thickness reduced and became less stable. The behavior and stabilization were different for the different sizes, with the correctly-sized generator in the lab seeming to be more affected by wind (possibly due to larger gaps or the particular wind direction in the lab), however the fire whirl

recovered much more clearly and quickly than the incorrectly-sized generator. While these tests did not conclusively show whether early extinguishment could be achieved with wind, it shows a direct influence of both wind and the apparatus geometry on stability of the fire whirl. Additional tests on this stability at larger scales with crude oil should be conducted to confirm precisely how external wind and changes in configuration size can influence the results, but were out of scope for the current project.

Fig. 51 Photos showing the influence of wind
Photos of a video from a correctly-sized triangular fire whirl generator over a 10 cm heptane pool fire. The center photo shows the flame decaying and attaching to the wall during external wind influences, which later recovers on the right hand side back to a fire whirl. Extinguishment is quick and brief.

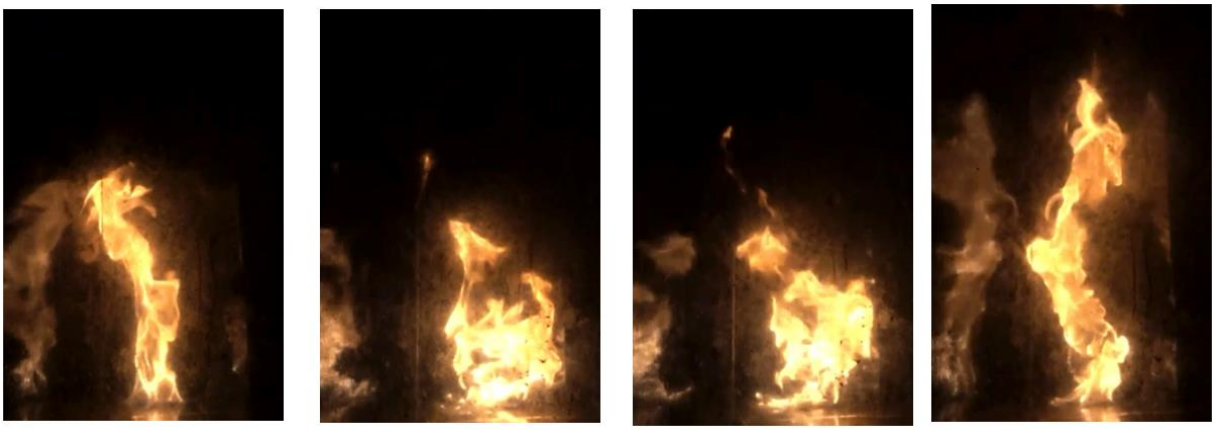

Fig. 52 Photos showing the influence of sizing and wind
Photos of a video from a triangular fire whirl generator sized to match closer large-scale experiments over a 10 cm heptane pool fire. The center 2 photos show the flame decaying and attaching to the wall during external wind influences, which later recovers on the right hand side back to a fire whirl. Extinguishment is quick and brief.

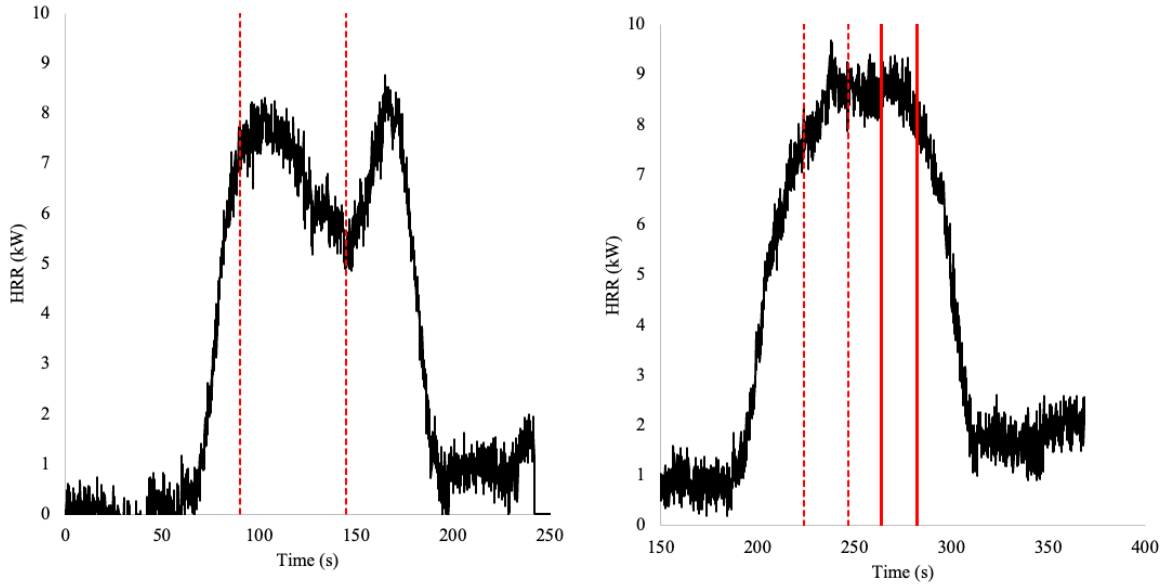

Fig. 53 Heat release rate for additional tests

The heat release rate measured from gas measurements of a 10 cm diameter fire whirl produced in the laboratory. The left hand side graph is generated by a correctly-sized triangular fire whirl generator and wind is applied between the vertical red dashed lines. The right-hand side graph is generated by a triangular fire whirl generator where the walls are placed closer to the fuel pan similar to large-scale experiments. The dips in HRR are more apparent for the correctly-sized fire whirl.

6 Conclusion and Future Research

6.1 Project Overview

All objectives in Phase I, II and III of the project were successfully completed. Phase I demonstrated that a three-wall fire whirl setup was the most efficient configuration that yielded the most stable and repeatable fire whirls. A tall wall configuration was necessary to provide the maximum benefit in terms of burning rate, efficiency, and reduced PM emissions, although this may make it more difficult to design an open-water apparatus in the future. However, it was interesting to note that low walls still produced some improved burning rates and efficiencies, however, it also produced higher PM emissions.

Phase II of the project investigated the effect of slick thickness utilizing the new three-wall fire whirl configuration, comparing emissions and efficiency results to the open pool fire configuration. As expected from Phase I and work from a previous project, fire whirls burned crude oil at both slick thicknesses at higher efficiencies, burning rates, and with overall reduced PM emissions. There were interesting effects observed in terms of boilover, however even under these conditions higher overall efficiency of burning was observed.

Phase III large-scale outdoor experiments were completed in May 2023 and demonstrated repeatable formation of fire whirls outdoors with large (1.5 m diameter) pools of crude oil. Results show reduced emissions, however, for some fire whirls fuel consumption efficiency was reduced. Comparing large-scale experiment to small-scale tests and literature data reveals the issue causing lower fuel consumption efficacy may lie with early extinguishment of the fire whirl. An exact mechanism causing this early extinguishment was not determined; however, it was suspected that both apparatus sizing and wind may play a role in the fire whirls destabilization near extinguishment. Overall concerns are justifiably raised about repeatability at large scale so more analysis on factors affecting stability and continued formation was conducted. Emissions data from the EPA was further analyzed. Analysis of ground-based measurements such as heat flux, flow, etc. were undertaken to compare small vs. large scale results.

6.2 Conclusions

In this project, laboratory small-scale and outdoor large-scale experiments were performed to characterize the effects of fire whirls vs. pool fires and slick thickness on burning efficiencies and emissions. To generate fire whirls, a new three-wall geometry was developed where gaps between the walls were oriented to induce swirling at the center of the test section. Investigations were performed to assess the configuration and dimensions that can most effectively form fire whirls over liquid fuels at the laboratory scale, where systems with three or four walls were arranged to restrict airflow. It was observed that the height and side length of the enclosure had an impact on the dynamics and formation of fire whirls. The optimal combinations of parameters from these experiments were assessed in terms of their effects on particulate emissions and modified combustion efficiency. The obtained results in this study confirm the feasibility of

using fire whirls with a three-wall setup for more efficient in-situ burning of crude oil spills and provide valuable information on the properties of fire whirls for deployment in the field.

Furthermore, laboratory and outdoor large-scale experiments were performed to investigate the influence of slick thickness on burning efficiency and emissions. The scalability of fire whirls from the laboratory to large-scale outdoor environments was successfully demonstrated. At all scales we found that compared to pool fires, fire whirls significantly increased the burning rate, while also reducing $PM_{2.5}$ emissions. By increasing the slick thickness from 3.8 mm to 11.5 mm in the laboratory, the burning rate increased more than 50% in fire whirls, with only a small change in pool fire conditions. Increasing the slick thickness in the laboratory also resulted in an increase in fuel consumption efficiency; nonetheless, it also increased emissions of $PM_{2.5}$. In the field, fuel consumption efficiencies of over 90% could be reached, however, for many fire whirl tests premature extinguishment of the ISB was observed lowering ultimate fuel consumption efficiencies. Results in the field were not very sensitive to fuel thickness. These experiments have helped to provide experimental evidence assessing the scalability, robustness, and efficiency of fire whirls in cleaning spilled oil, and help to highlight issues on stability and premature extinguishment needing further study.

6.3 Technology Development

This project was designed to serve as a proof-of-concept at BSEE technology readiness level (TRL) 5, a technology prototype tested in relevant environments, to suggest opportunities and modifications to future designs for commercial implementation. While the apparatus was tested at this stage, more questions have arisen, in particular related to stability of fire whirls near extinguishment, needing further study before proceeding to TRL 6. Further, the proposed design does not have feasible plans actionable by commercial entities, as of yet, for open-ocean implementation. Tall walls were necessary to achieve improved emissions reductions but these also may pose challenges when designing a floating platform. In regards to the requested schematics of the design, Figure 34 shows the specific dimensions of the large-scale configuration used for the demonstration at TEEX. As discussed earlier, the test ring and wall dimensions did not match the specifications given to TEEX so there was too short a distance between the wall and fuel pool, affecting results. Therefore, further testing is needed before the technology can be truly assessed for a commercialization plan and final schematics of a field-implementable configuration can be provided. These results have provided critical information necessary to further development before moving to commercial applications.

6.4 Conferences and Publications

Below is a list of conferences and publications already submitted, accepted or presented:

- Experimental Characterization of Enhanced In-situ Burning Using Fire Whirls on a Three-wall Structure, Joseph L. Dowling, Mohammadhadi Hajilou, Michael J. Gollner,

43rd AMOP Technical Seminar June 8-10 in Edmonton (Canada). Paper Accepted, Presented, and in Proceedings

- The effect of enclosure dimensions on fire whirl formation and emissions, J.L. Dowling, M. Hajilou, M.J. Gollner, 2022 Spring Technical Meeting of the Western States Section of the Combustion Institute, Stanford University – Stanford, CA March 21-22, 2022. Abstract Accepted for Presentation and Presented
- Development of Large-Scale Fire Whirls for Offshore Oil Spill Cleaning, Mitchell Huffman, Joseph Dowling, Bhushan Pawar, Wuquan Cui, Mohammadhadi Hajilou, Karen Stone, Elaine Oran, Michael J. Gollner, Qingsheng Wang, 2023 AIChE Annual Meeting, November 5-10, 2023, Orlando, FL. Abstract Accepted for Presentation and Presented
- Effects of Fuel Layer Slick Thickness on Fire Whirl Emissions and Burning Rate, J.L. Dowling, W. Cui, J. Tan, M.J. Gollner, 2023 Fall Technical Meeting of the Western States Section of the Combustion Institute, CSU Northridge – Northridge, CA October 16-17, 2023. Abstract Accepted for Presentation and Presented
- Multi-scale Experimental Characterization of In-situ Burning Using Fire Whirls and the Effect of Oil Slick Thickness on Burning Efficiencies and Emissions, Joseph L. Dowling, Mohammadhadi Hajilou, Wuquan Cui, Mitchell Huffman, Bhushan Pawar, Elaine Oran, Qingsheng Wang, Karen N. Stone, Michael J. Gollner, International Oil Spill Conference, May 13 - 16, 2024, New Orleans, Louisiana. Abstract Accepted and Proceeding Paper Submitted

6.5 Future Research

While the research tasks were completed, new questions have arisen and potential opportunities to pursue additional approaches to improve ISB of oil that can be pursued. First and foremost, the large-scale outdoor experiment in Texas demonstrated both the feasibility of the approach but also its sensitivity to environmental factors and small changes to apparatus dimensions affecting the burning behavior. These are real issues that could be encountered in practical use of this or other approaches. The sensitivity of the apparatus at small scale was at first improved using the three-walled setup; however, the influence of external wind, changes in dimensions, different fuel properties, waves, etc. may play an important role that has not yet been characterized and deserves further study.

As with all fire research, scaling results from the laboratory to the field is always a challenge. Laboratory experiments have helped to guide this work and optimize the number of tests to be performed in the field, however continued study at large scale will be necessary to fully understand the observed behavior and prepare a prototype ready for open ocean operation.

An overarching observation from this and related studies on ISB has been that increases in efficiencies are possible when modifying conditions that affect the fire. First, increasing heat fluxes to the fuel surface, such as is achieved by changing the geometry of the fire whirl has a direct benefit on increasing the burning rate. Similar improvements can be found in other approaches such as the Flame Refluxer (also funded by BSEE (Rangwala et al. 2021)) which uses a metal substrate in the oil layer to increase heating. Larger pool fires are also limited in efficiency by a lack of available oxygen near the center of the fuel pool. Enhancing ventilation

has the possibility of reducing airborne emissions. EPA studies of different configurations of oil spills including line configurations reduced emission factors of soot (Aurell et al. 2021). Fire whirls are remarkably adept as they can achieve both of these conditions (enhanced ventilation and heating of the fuel pool) without exterior mechanical ventilation. However, we have seen stability affects the formation and continuation of fire whirls that could pose a problem with their implementation if not studied and accounted for. Unfortunately, there were not enough large scale experiments to explore these issues. There is a possibility that mechanically inducing circulation, either through fans, a more enclosed configuration, other means, could enhance the stability of these processes or even other related configurations to a point that they achieve all objectives. This should be studied in future research and eventually replicated at scale.

One of the most interesting observations, both at small and large scale, had to do with the process of boilover. While often cited that boilover does not occur at large scale, overturning of the pool was observed at large scale, but not perhaps as vigorously as occurred in the laboratory. Laboratory measurements of boilover indicated that much more rapid mass loss occurs and, although instantaneous emissions are greatly enhanced, overall emission factors per unit fuel consumed do not vary much. This leads to the potential of encouraging boilover to occur to enhance fuel burning efficiencies.

Boilover is a complex process that is not yet well understood. During this process there are multiple phases changing and reacting at the same time, with interactions specifically between the water, oil layer, and gases above being incredibly complex. The surface tension of the oil affects the ability for droplets of oil to form, which then burn more vigorously, and the effect of a different burning configuration on rates, heating, emissions, etc. is not well understood. Physically studying this process for a wide range of oils and burning conditions would greatly enhance our ability to use this process effectively in ISB operations.

Observation of a significant reduction in soot emissions when burning as a fire whirl highlights how changes in flow may affect emissions. Our understanding of this process, however, has barely scratched the surface. There are interesting remaining questions on how these conditions in the gas phase effects emissions of soot and other compounds from a more fundamental standpoint. This understanding could help guide configurations and conditions to reduce harmful emissions in the future. Furthermore, the oil layer changes during burning yet the makeup of residue is largely unknown until after the burning completes. Studying changes of the chemistry of burning residue with time would also be of interest both to enhance burning efficiencies and understand potential pollutant effects.

A lack of fundamental understanding still exists, in part because expansive diagnostics, even for small scale experiments with crude oil, are difficult to implement. Numerical simulations offer an opportunity to further probe both current and future conditions. These simulations can attempt to replicate existing experimental data and inform the processes that are occurring that cannot be seen or measured in experiments, then modified to optimize conditions in the future. Observations such as foams or “frothing” in some oil experiments have yet to be explained but multi-phase simulations may be able to get at the physics of these issues and enhance our understanding.

7 References

Allen AA, Ferek RJ. 1993. Advantages and disadvantages of burning spilled oil. International Oil Spill Conference Proceedings. 1993(1):765-772.

Aurell J, Holder A, Gullett B, Lamie N, Arsava K, Conmy R, Sundaravadivelu D, Mitchell W, Stone KJMPB. 2021. Analysis of emissions and residue from methods to improve efficiency of at-sea, in situ oil spill burns. 173:113016.

Bech C, Sveum P, Buist I. 1992. In-situ burning of emulsions: The effects of varying water content and degree of evaporation. Canada. No. 0-662-59050-3.

Brogaard N, Sørensen M, Fritt-Rasmussen J, Rangwala A, Jomaas G. 2014. A new experimental rig for oil burning on water – results for crude and pure oils. Fire Safety Science. 11:1481-1495.

Buist I. 2003. Window-of-opportunity for in situ burning. Spill Science & Technology Bulletin. 8(4):341-346.

Buist I, Potter S, Nedwed T, Mullin J. 2011. Herding surfactants to contract and thicken oil spills in pack ice for in situ burning. Cold Regions Science and Technology. 67(1):3-23.

Buist I, Trudel K, Morrison J, Aurand D. 1997. Laboratory studies of the properties of in-situ burn residues. International Oil Spill Conference Proceedings. 1997(1):149-156.

Cooperman P. 2004. Some criteria for the in situ combustion of crude oil. Journal of Applied Physics. 30(9):1376-1380.

Fay JA. 1969. The spread of oil slicks on a calm sea. In: Hoult DP, editor. Oil on the sea: Proceedings of a symposium on the scientific and engineering aspects of oil pollution of the sea, sponsored by massachusetts institute of technology and woods hole oceanographic institution and held at cambridge, massachusetts, may 16, 1969. Boston, MA: Springer US. p. 53-63.

Fingas M. 2019. Marine oil spills 2018. MDPI.

Fingas MF, Halley G, Ackerman F, Nelson R, Bissonnette M, Laroche N, Wang Z, Lambert P, Li K, Jokuty P et al. 1995. The newfoundland offshore burn experiment—nobe. International Oil Spill Conference Proceedings. 1995(1):123-132.

Garo J, Vantelon J, Gandhi S, Torero JJSS, Bulletin T. 1999. Determination of the thermal efficiency of pre-boilover burning of a slick of oil on water. 5(2):141-151.

Gelderen, L., & Jomaas, G. 2017. The parameters controlling the burning efficiency of in-situ burning of crude oil on water. 2017.

Gollner M, Oran E, Hariharan S, Dowling J, Farahani H, Rangwala AJBoS, Enivronmental Enforcement TR. 2019. Efficient remediation of oil spills over water using fire whirls (project number 1094).

Hariharan SB, Farahani HF, Rangwala AS, Dowling JL, Oran ES, Gollner MJ. 2021. Comparison of particulate-matter emissions from liquid-fueled pool fires and fire whirls. Combustion and Flame. 227:483-496.

Hobbs JLRRJF, Peter V. 1996. Particle and gas emissions from an in situ burn of crude oil on the ocean. Journal of the Air & Waste Management Association. 46(3):251-259.

Hoult DP. 1972. Oil spreading on the sea. 4(1):341-368.

Hurley MJ, Gottuk DT, Hall Jr JR, Harada K, Kuligowski ED, Puchovsky M, Watts Jr JM, WIECZOREK CJ. 2015. Sfpe handbook of fire protection engineering. Springer.

IPIECA IJL, UK. 2016. In-situ burning of spilled oil-good practice guidelines for incident management and emergency response personnel.
Law RJ, Hellou JJEG. 1999. Contamination of fish and shellfish following oil spill incidents. 6(2):90-98.
Lin Q, Mendelssohn IA, Carney K, Miles SM, Bryner NP, Walton WD. 2005. In-situ burning of oil in coastal marshes. 2. Oil spill cleanup efficiency as a function of oil type, marsh type, and water depth. Environmental Science & Technology. 39(6):1855-1860.
Luketa A. 2018. Fire whirl investigation. United States.
Guidance on burning spilled oil in situ. 1995. Office of Response and Restoration; [accessed]. https://response.restoration.noaa.gov/oil-and-chemical-spills/oil-spills/resources/insitu-burning.html.
Peters MA. 2017. Oil geopolitics and eco-nightmares. Educational Philosophy and Theory. 49(5):435-438.
Peterson CH, Rice SD, Short JW, Esler D, Bodkin JL, Ballachey BE, Irons DB. 2003. Long-term ecosystem response to the exxon valdez oil spill. 302(5653):2082-2086.
Rangwala A, Arsava K, Sauer N, Ho H, Nair S, Mahnken G, Kottalgi M. 2021. Advancing the maturity of the flame refluxer technology. Us department of the interior, bureau of safety and environmental enforcement report no: 1104 contract no: 140e0118r0007.
Ross HD. 1994. Ignition of and flame spread over laboratory-scale pools of pure liquid fuels. Progress in Energy and Combustion Science. 20(1):17-63.
Teal JM, Howarth RW. 1984. Oil spill studies: A review of ecological effects. Environmental Management. 8(1):27-43.
Torero JL, Olenick SM, Garo JP, Vantelon JP. 2003. Determination of the burning characteristics of a slick of oil on water. Spill Science & Technology Bulletin. 8(4):379-390.
Gelderen L, Brogaard NL, Sørensen MX, Fritt-Rasmussen J, Rangwala AS, Jomaas G. 2015. Importance of the slick thickness for effective in-situ burning of crude oil. Fire Safety Journal. 78:1-9.
Walavalkar AY, Kulkarni AK. 2001. Combustion of water-in-oil emulsion layers supported on water. Combustion and Flame. 125(1):1001-1011.
Wu N, Baker M, Kolb G, Torero JL. 1996. Ignition, flame spread and mass burning characteristics of liquid fuels on a water bed. Spill Science & Technology Bulletin. 3(4):209-212.
Wu N, Kolb G, Torero JL. 1998. Piloted ignition of a slick of oil on a water sublayer: The effect of weathering. Symposium (International) on Combustion. 27(2):2783-2790.
Xiao H, Gollner MJ, Oran ESJPotNAoS. 2016. From fire whirls to blue whirls and combustion with reduced pollution. 113(34):9457-9462.
Zock J-P, Rodríguez-Trigo G, Pozo-Rodríguez F, Barberà JA, Bouso L, Torralba Y, Antó JM, Gómez FP, Fuster C, Verea HJAjor et al. 2007. Prolonged respiratory symptoms in clean-up workers of the prestige oil spill. 176(6):610-616.

Appendixes

Appendix A: Technical Summary

REPORT TITLE: Efficient Remediation of Oil Spills Using Fire Whirls

CONTRACT NUMBER(S): 140E0121C0004

FISCAL YEARS(S) OF PROJECT FUNDING: 2020, 2021, 2022, 2023

CUMULATIVE PROJECT COST: $864,220.00

COMPLETION DATE OF REPORT: 14 December 2023

BSEE COR(S): Karen Stone

BSEE CO(S): Caroline Laikin-Credno

PROJECT MANAGER(S): Michael J Gollner

AFFILIATION OF PROJECT MANAGER: University of California, Berkeley

ADDRESS: University Avenue, Berkeley, CA 94720

PRINCIPAL INVESTIGATOR(S)*: Michael J Gollner

KEY WORDS: In-Situ Burning, Oil Spill, Fire Whirl, Slick Thickness, Mass Loss, Fuel Consumption Efficiency, Emission, Boilover, Large Scale Experiment, Three-Wall Protocol

Department of the Interior (DOI)
The Department of the Interior protects and manages the Nation's natural resources and cultural heritage; provides scientific and other information about those resources; and honors the Nation's trust responsibilities or special commitments to American Indians, Alaska Natives, and affiliated island communities.

Bureau of Safety and Environmental Enforcement (BSEE)
The mission of the Bureau of Safety and Environmental Enforcement works to promote safety, protect the environment, and conserve resources offshore through vigorous regulatory oversight and enforcement.

BSEE Oil Spill Preparedness Program
BSEE administers a robust Oil Spill Preparedness Program through its Oil Spill Preparedness Division (OSPD) to ensure owners and operators of offshore facilities are ready to mitigate and respond to substantial threats of actual oil spills that may result from their activities. The Program draws its mandate and purpose from the Federal Water Pollution Control Act of October 18, 1972, as amended, and the Oil Pollution Act of 1990 (October 18, 1991). It is framed by the regulations in 30 CFR Part 254 – *Oil Spill Response Requirements for Facilities Located Seaward of the Coastline*, and 40 CFR Part 300 – *National Oil and Hazardous Substances Pollution Contingency Plan*. Acknowledging these authorities and their associated responsibilities, BSEE established the program with three primary and interdependent roles:

- Preparedness Verification,
- Oil Spill Response Research, and
- Management of Ohmsett - the National Oil Spill Response Research and Renewable Energy Test Facility.

The research conducted for this Program aims to improve oil spill response and preparedness by advancing the state of the science and the technologies needed for these emergencies. The research supports the Bureau's needs while ensuring the highest level of scientific integrity by adhering to BSEE's peer review protocols. The proposal, selection, research, review, collaboration, production, and dissemination of OSPD's technical reports and studies follows the appropriate requirements and guidance such as the Federal Acquisition Regulation and the Department of Interior's policies on scientific and scholarly conduct.